HIGH-LATITUDE GEOMAGNETIC VARIATIONS AND SUBSTORMS

V. M. MISHIN

Siberian Institute of Terrestrial Magnetism, Ionosphere and Radio Wave Propagation, Irkutsk, U.S.S.R.

Abstract. The present review concerns high-latitude geomagnetic variations, and in particular those caused by fluctuations of the interplanetary magnetic field. It is shown that IMF B_z, B_x, B_y and $|B_y|$ produce four kinds of geomagnetic effects, which qualitatively agree with the expected consequences of the reconnection hypothesis. At quiet time the cleft into the Earth's magnetosphere has a quasi-circular shape at $\Phi \approx 78°$ that also fits qualitatively the reconnection model by Stern (1973) but does not agree with the conception of *dayside* cusps.

From the analysis of the geomagnetic effects of IMF B_z it was found also that the contribution of magnetospheric dynamo to the electric field of the dayside plasmasphere (middle and low latitudes) does not exceed 15–20%. Characteristics of this contribution are given (i.e. *DP*-2 fields).

The magnetic substorm models are reviewed as well. Geomagnetic data confirm the existence of the substorm growth phase both at $B_z < 0$ and at $B_z > 0$. The expansion phase of most substorms evidently involves the processes of reconnection and neutral line formation near the inner edge of the plasma sheet ($LT \approx 23^h$), resulting from instability of field-aligned currents of the westward electrojet at $h \sim 1000$ km. Such a mechanism accounts for a number of signatures for local development of substorms, including coastal effect, jumplike development of the electrojet, etc. The second kind of substorms, not involving the magnetic disturbances, is probably caused by the development of ion tearing instability in the plasma sheet.

The original results are presented against a general review background, which includes a method for mathematical description of global fields of magnetic variations and substorms.

Contents

1. Introduction

Geomagnetic variations within the period range 10^2–10^4 s are one of the most studied geophysical phenomena. This is inferred, first of all, from the fact that continuous recording of variations has been performed for more than a century, thanks to the relative simplicity and low cost of ground magnetometers.

Ground-based geomagnetic variations provide a significant part of general information about the state of the Earth's magnetosphere and, in particular, key information about the coupling of magnetospheric convection and electrical fields

Space Science Reviews **20** (1977) 621–675.

with the interplanetary magnetic field. They contribute much to the modern concept of a magnetospheric substorm, showing, for instance, strong evidence (as opposed to auroral data) for the existence of a growth phase and other characteristics of substorm development within the magnetosphere. In addition to the complex of ground-based and satellite data, geomagnetic observations improve our knowledge of the space–time distribution of streams of trapped and precipitated particles in the magnetosphere, and the model of the geomagnetosphere. In particular, these data point to the existence of the closed (i.e. observed at all LT-meridians) magnetospheric cleft – a main channel of solar wind plasma injected into the geomagnetosphere.

The above stated problems are the chief subject of the present paper.

Many results presented in this paper are obtained mainly through the synthesis of data from a network of ground-based magnetic stations – world-wide or high-latitude ones ($\Phi \geqslant 60°$). This network is rather sparse and nonuniform. For this reason the solution of the problem of such a synthesis is of special interest and is briefly described in the first section. The second section is concerned with the selected results of the study of geomagnetic variations, electric fields and currents in the quiet geomagnetosphere. The third deals with magnetic substorms. The original results referred to in these sections are presented against a general review background.

2. A Method for Mathematical Description of a Geomagnetic Variation Field

It is known that magnetic measurements at the Earth's surface may be described analytically in terms of the Gauss theory according to which

$$V = a \sum_{n=1}^{\infty} \sum_{m=0}^{n} [T_n^m \cos mt + i_n^m \sin mt][a/(a-h)]^{n+1} \times P_n^m(\cos\theta)$$
$$+ a \sum_{n=1}^{\infty} \sum_{m=0}^{n} [E_n^m \cos mt + e_n^m \sin mt][(a+h)/a]^n \times P_n^m(\cos\theta); \quad (1.1)$$

$$-\mathbf{grad}\ V = \mathbf{F}, \quad \mathbf{F} = \mathbf{iX} + \mathbf{jY} + \mathbf{kZ}, \quad (1.2)$$

where a is the Earth's radius, h is the height over the Earth's surface, t is longitude in hours, θ is the colatitude, and $\mathbf{F}$ is the field vector.

Description with the help of (1.1) enables us, in principle, not only to synthesize a great number of discrete geomagnetic measurements but to divide their fields into portions caused by the outer and inner (with respect to the Earth's surface) sources, and also to calculate the current function

$$T_e = -(4\pi/10) \sum_{n=1}^{\infty} \sum_{m=0}^{n} (2n+1)/(n+1)[(a+h)/a]^n$$
$$\times (E_n^m \cos mt + \boldsymbol{e}_n^m \sin mt) P_n^m(\cos\theta), \quad (1.3)$$

i.e. to construct two-dimensional systems of electrical currents equivalent to fields $F(\theta, t)$.

In practice, the calculation of coefficients in (1.1) and (1.3) is a solution of systems of linear algebraic equations which are derived from (1.1) and (1.2) and have the form:

$$F_l(X_i) = \sum_{K=1}^{R} d_K G_K(X_i). \tag{1.4}$$

Here F_l is the measured value of one in three rectangular components of vector F, $G_K(X)$ – Legendre polynomials and their derivatives with some factors.

Each of the Equations (1.4) is satisfied approximately and d_K is an approximate value of of Fourier coefficient d_K^0. The following relation takes place:

$$\delta_i F_l(X_i) - \sum_{K=1}^{R} d_K G_K(X_i) = \sum_{K=R+1}^{\infty} d_K^0 G_k(X_i) + \sum_{K=1}^{R} (d_K - d_K^0) G_K(X_i) + \Delta_i, \tag{1.5}$$

where Δ_i is an error of measurement in point X_i of component F_l, $i = \overline{1, N}$, N is a number of measurement points.

System (1.4) is solved by the least-squares method, so that

$$\|\sigma\| = \min. \tag{1.6}$$

Under such a generally accepted statement the solution of (1.4) requires giving a spectrum of functions $G_K(X)$. This circumstance (which attracted no attention earlier, while analyzing a main geomagnetic field), appears to be decisive when describing the geomagnetic variation fields even for such simple events as the instantaneous S_q-field. Therefore, Mishin and Bazarzhapov (1966), following Fougere (1963), have optimized a selection of functions G_K in (1.4), using their canonical sequence. On the basis of the latter, functions $\Phi_K(X)$, orthogonal at a set of points $\{X_i\}$, were introduced and a system of equations like

$$F_l(X_i) = \sum_{K=1}^{R} a_K \Phi_K(X_i) \tag{1.4'}$$

was solved. Then values d_K were computed, using the coefficient a_K. However, at this step, an additional condition was introduced:

$$\left| \frac{\Delta a_K}{a_K} \right| < 1, \tag{1.7}$$

where Δa_K is an estimation of an error of coefficient a_K. This condition follows from the requirement:

$$\sum_{K=R+1}^{\infty} \left\| d_K^0 G_K(X_i) \right\| = \min. \tag{1.8}$$

If some coefficients a_K did not satisfy condition (1.7), they were assumed to equal zero and the corresponding functions were eliminated from approximating series

(1.4′) and (1.4). Thereby, a selection of approximating functions was ensured for the following purpose:

(1) to choose functions G_K, bearing the principal information on field $\mathbf{F}(\theta, t)$;

(2) to minimize the deviations from orthogonality of vectors G_K at a set of points $\{X_i\}$, which provides the interdependence of coefficients d_K and increases differences $|d_K - d_K^0|$.

The above-stated procedure directly solves problem 2 and indirectly, through the selection of functions Φ_K, problem 1.

As was shown (see e.g. Mishin *et al.*, 1971), condition (1.7) ensures the accuracy of definition (1.3), sufficient for description of instantaneous S_q-fields and those of S_q^P-type. When describing substorm fields, this method was modified by Bazarzhapov *et al.* (1975). In this modification the role of a canonical sequence of functions G_K as a basis for selection of the approximating spectrum of these functions was essentially diminished though the initial, as before, were conditions (1.6), (1.8) and condition

$$R \leq R_0, \tag{1.9}$$

implying that the 'wavelength' of the relevant functions is not less than the shortest distance between points X_i.

Instead of a canonical sequence of functions G_K Bazarzhapov *et al.* (1975) have used the sequence of such functions, obtained after computation and re-ordering of 'contributions' of functions G_K into field $\mathbf{F}(\theta, t)$ according to their diminution. 'Contributions' were estimated by formulae:

$$\|d_K G_K\| = [(d_K G_K(X_1))^2 + (d_K G_K(X_2))^2 + \cdots + (d_K G_K(X_N))^2]^{1/2}$$

$$d_K = (F_l, G_K)/(G_K, G_K).$$

From a series of contributions $\|d_K G_K\|$, ordered initially in a canonical sequence, the greatest one was chosen and it (and the corresponding function G_K) was designated as number 1. Then the difference $F_l - d_1 G_1$ was examined, the greatest contribution was found for it, and the corresponding function G was numbered 2. In such a manner selection was made of the sequence of functions G_K which subsequently replaced a canonical one. In this way problem 1, stated above, was directly solved.

Such a method for selection of approximating functions has appeared to be effective enough. In particular, it has permitted inferring originally the analytical representation of ground magnetic substorm fields and of fields δ_Y, described below.

3. Quiet Variations

3.1. Fields and currents S_q^P, DP-2 – effects of B_Z- and B_Y-components of the IMF

3.1.1. In middle latitudes there are well-known quiet solar-diurnal geomagnetic S_q-variations, caused,as was generally accepted until recently, for the most part by

the dynamo-action of neutral winds in the ionospheric E-region. Nagata and Mizuno (1955) as well as Nagata and Kokubun (1962) have shown that in high latitudes there is a field $S_q^P = S_q - S_q^0$ along with S_q^0, which is an analytical continuation of the midlatitude S_q-field. Two-dimensional systems of currents, equivalent to the S_q^P-field, are shown in Figure 1.

These patterns are obtained by averaging the data of international quiet days, i.e. they correspond to mean quiet conditions. On the other hand, the data of direct measurements show that the electric field in the quiet polar ionosphere has the form shown in Figure 2a, i.e. it is produced by the anti-solar plasma convection in the outer portion of the magnetosphere which is projected onto the polar caps ($\Phi \geqslant 75°$), and by the sunward convection within $\Phi < 75°$. Comparing the data of Figures 1 and 2a, we suggest that the two-dimensional equivalent S_q^P-currents be considered, in the main, as Hall currents in the E-region of the polar ionosphere.

A total system of S_q^P-currents, corresponding to the electric field in Figure 2a and to high electroconductivity along the geomagnetic field lines, should be essentially a three-dimensional one. As seen from Figure 2b it involves, apart from a two-vortex system of Hall currents, at least one other, i.e. a system of Pedersen and of closing field-aligned currents. However, ground magnetic fields of Pedersen currents and of field-aligned ones can be assumed to be mutually compensated insofar as the geomagnetic field lines in high latitudes are close to vertical ones and electroconductivity nonuniformities may be neglected. Thus, the main ground-based effect would be produced by Hall currents (Fukushima 1969).

For this reason the equivalent S_q^P currents are mostly the polar ionospheric Hall ones, reflecting a two-vortex system of magnetospheric plasma convection. The existence of such convection systems, of the dawn–dusk electric field and Hall currents, was predicted by Axford and Hines (1961) and by Dungey (1961), respectively, on the basis of viscous friction and reconnection hypotheses. According to the former, the S_q^P-currents may occur even if no IMF is assumed to exist; according to the latter, they are enhanced with an increasing south IMF component, and the module of Y-component (Nishida 1971; Stern 1973; Gonzalez and Mozer 1974; Matveev and Mishin 1975; Ivanov and Evdokimova, 1975). So, the dawn–dusk electric field in the linear approximation is $E = E_0 + K_I B_S + K_2 |B_Y|$, where E_0 is a contribution of viscosity. According to approximate estimations by Gonzalez and Mozer (1974) and by Mozer *et al.* (1974) we have $K_1 \approx 3$ mv m, γ^{-1}, $(K_1/K_2) \approx 2$. Let us try to clarify whether these estimates are supported by the data of geomagnetic variations.

To answer this question, Mishin *et al.* (1975c) have studied the dependence of values $E = T/\bar{\Sigma}_H$ on the IMF B_S, where T is a total current S_q^P flowing across the polar cap, and $\bar{\Sigma}_H$ is the Hall conductivity after Osipova and Vanjan (1975)* . The data of 8 quiet summer days (days of 1968 with $|B_Y| \approx 2.5\gamma$) were used. The

* The line above means the average over the polar cap area $\Phi \geqslant 75°$).

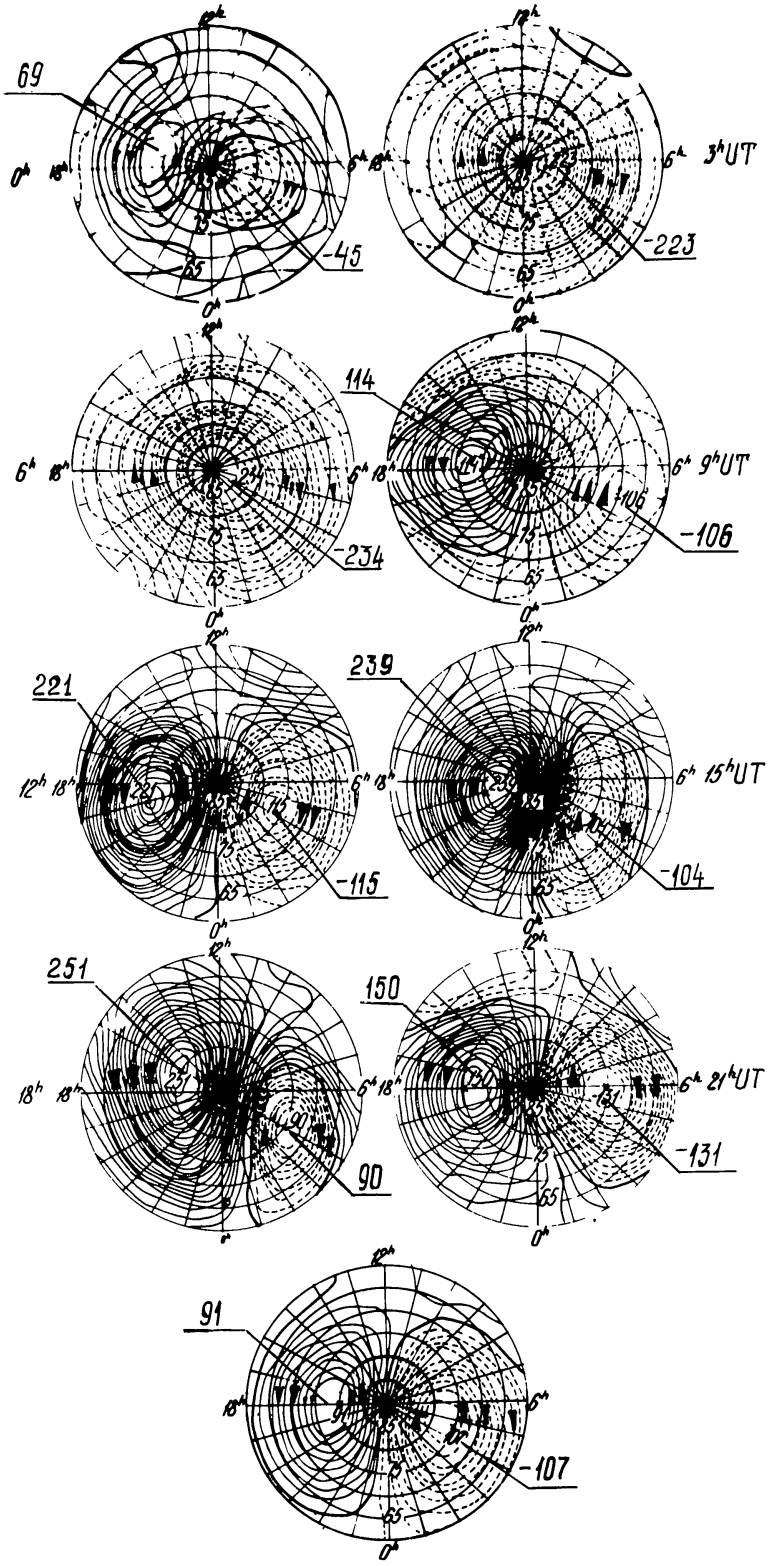

Fig. 1. Systems of equivalent S_q^P-currents at different UT-moments (shown to the left and to the right along the vertical). *Bottom:* the averaged current system in geomagnetic coordinates latitude-time. Focal values – in kiloamperes. (V-VIII, 1958, N-Hemisphere).

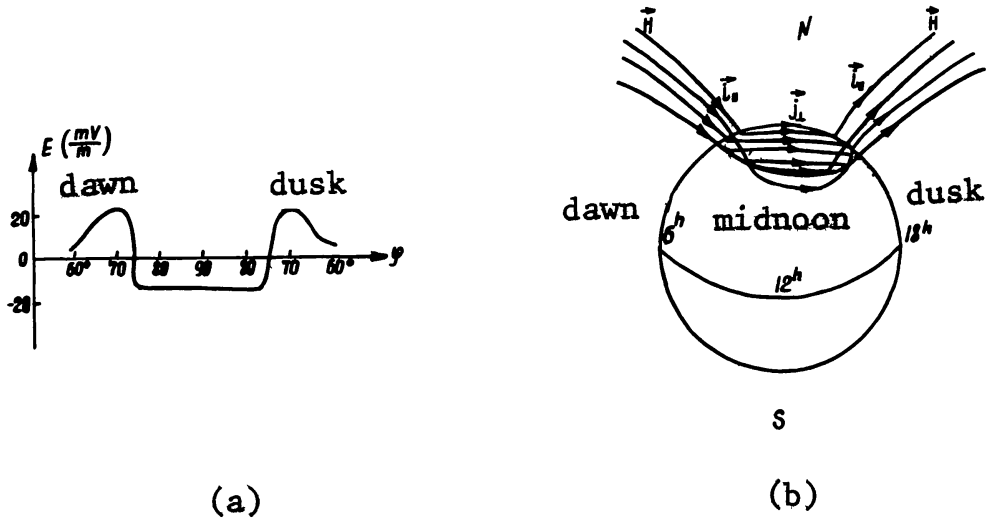

Fig. 2. (a) Model distribution of the 'dawn–dusk' electric field along the 6–18^{h}LT-meridian in the polar cap. (b) A three-dimensional system of S_q^P-currents, involving ionospheric Pedersen currents and field-aligned ones (without Hall currents).

results are shown in Figure 3, to which correspond the estimations:

$$E_0 \approx (3\text{–}6)\text{mv m}^{-1}\ K_1 \approx (2.5\text{–}5)\text{mv m}\gamma^{-1};\ K_2 \approx (2\text{–}3)\text{mv m}\gamma^{-1}.$$

The relation (K_1/K_2) can be determined also on data from Figure 4, taken from work by Friis–Christensen and Wilhjelm (1974, Figure 10). It illustrates the dependence from IMF B_Z of the magnetic field component h_2 in Thule, reckoned from the zero IMF level ($|B_Z|<1\gamma$ and $|B_Y|<1.5\gamma$). Component h_2 is chosen so that it is proportional to the 'dawn–dusk' electric field. The reference level

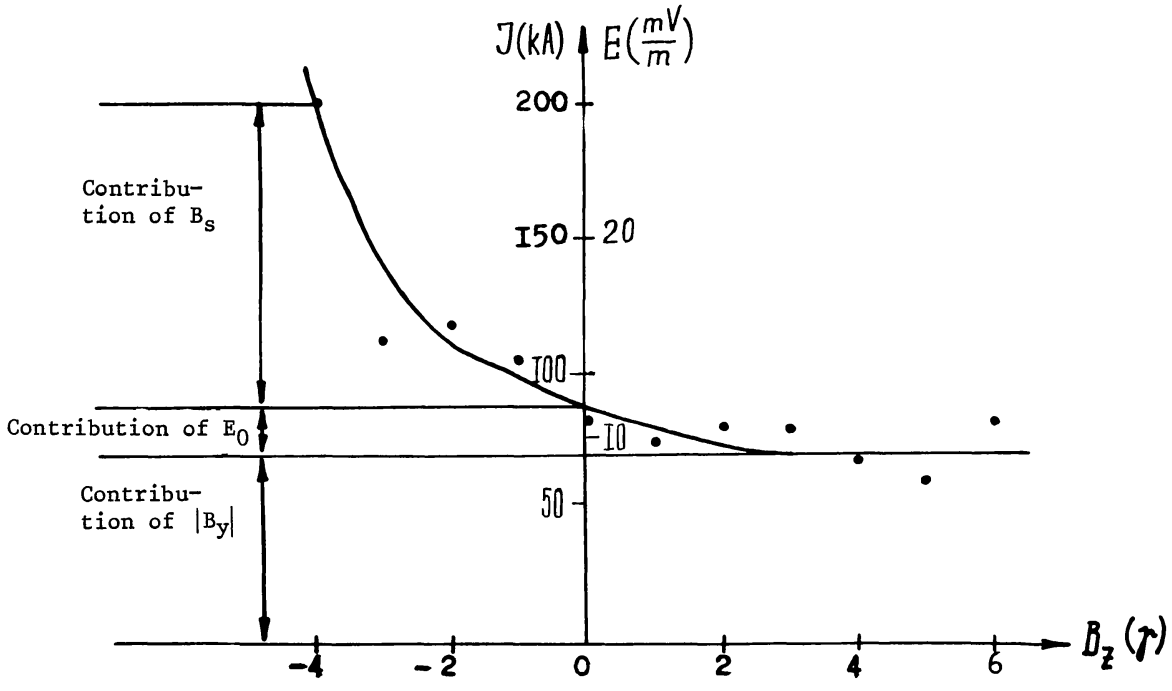

Fig. 3. The intensity of S_q^P-currents as a function of IMF B_z-component. The expected contributions of B_s, $|B_y|$ and E_0 are marked.

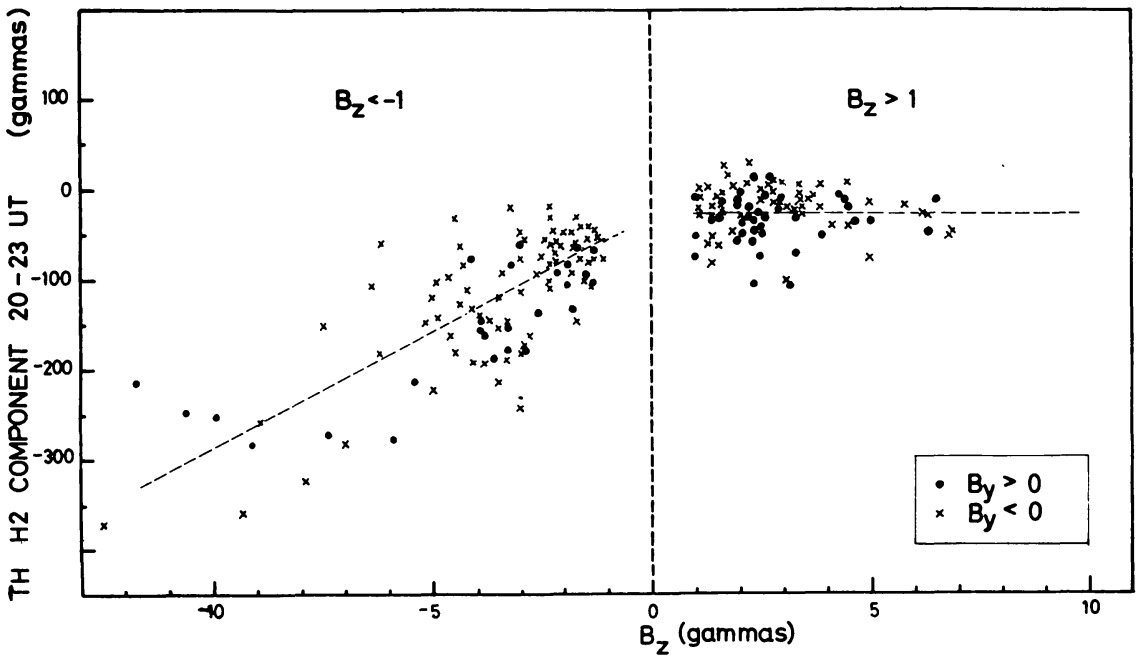

Fig. 4. Variations of the horizontal H_2 component in Thule at 20–23^{h}UT as a function of IMF B_z-component. Values ΔH_2 are proportional to the 'dawn–dusk' electric field, (after Friis–Christensen and Wilhjelm (1974)).

provides the elimination of the part E_0. Therefore, a systematic deviation of h_2 from zero in the entire region $B_Z > 0$ (see Figure 4) is unambiguously interpreted as the effect of IMF $|B_Y|$. This effect, as seen, does not depend on sign B_Y so that $h_2 \approx C_1 B_S + C_2 |B_Y|$. Assuming $|B_Y| = (3 \pm 1)\gamma$ we find from Figure 5 $(C_1/C_2) = (25/10)$–$(25/30)$.

So the estimations obtained from geomagnetic data are approximately consistent with the theoretical estimated value $(K_1/K_2) \geq 2$. Hence, in production of the main 'dawn–dusk' electric field, whose enhancement gives rise to substorm development, both components B_S, $|B_Y|$ of the IMF play significant roles along with the viscous interaction (the latter varying with the rate at which plasma is brought up to the front of the magnetosphere).

As mentioned already, the existence of a strong dependence of the two-vortex convection and the 'dawn–dusk' electric field upon $|B_Y|$ follows from theoretical considerations. From merely qualitative reasoning inferred from the reconnection hypothesis, such a dependence was predicted by Nishida (1971) and by Matveev and Mishin (1975) (Figure 5). Having postulated the magnetopause reconnection, Stern (1973) computed a magnetic field produced by the superposition of the constant solar wind magnetic field onto that of a geomagnetic dipole, and determined the distribution of the solar wind electric field projection $-\mathbf{V} \times \mathbf{B}_Y$ in the polar ionosphere assuming the geomagnetic field lines to be equipotentials. It appears that in the polar cap ionosphere the field $-\mathbf{V} \times \mathbf{B}_Y$ has a 'dawn-to-dusk' directed component regardless of sign B_Y; this contribution to the dawn–dusk electric field, due to the Y-component of the IMF, is comparable with that for the

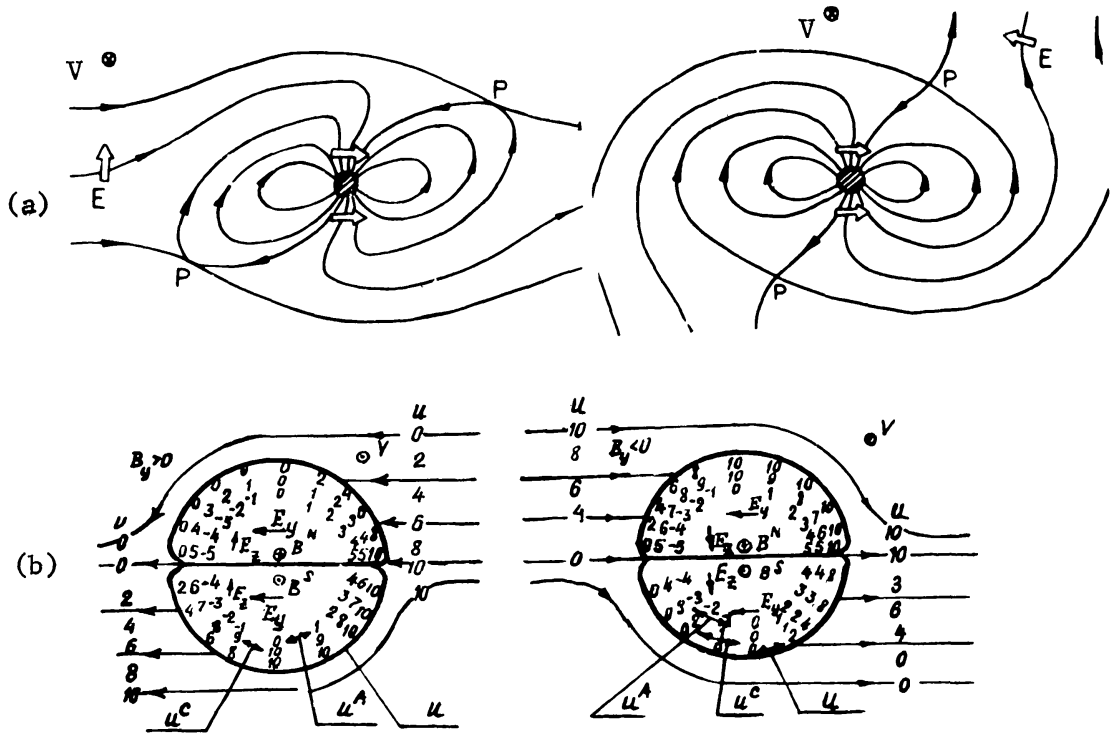

Fig. 5. Reconnection models after Nishida (1971) (a) and Matveev and Mishin (1975) (b). The bottom panel shows a cross-section of the tail, magnetic field lines and distribution of the U-potential of field $-\mathbf{V}\times\mathbf{B}_y$. The upper row of ciphers – values U; the middle – its part U^c, symmetric with respect to Y-axis; the bottom – antisymmetric part of potential U^A. Arrows show the direction of fields $E_y = -\text{grad } U^c$ and $E_z = -\text{grad } U^A$. Field E_y in each of the bottom patterns is directed, irrespective of sign B_y, from dawn to dusk, as shown in Figure 5a. A sign of field E_2 depends on B_y. (*Top:* view from the Sun; *bottom:* view from the tail).

B_Z-component (Figure 6). The expected contribution of the Y-component to the above field is noted also in work by Gonzalez and Mozer (1974) and by Ivanov and Evdokimova (1975). These works are based on the reconnection hypothesis so that data of Figures 3 and 4 are the new argument in favor of magnetopause reconnection and of the decisive role of this process in production of main electric fields in the outer magnetosphere and in the polar ionosphere.

3.1.2. Figure 3 is of interest as well for the theory of midlatitude Sq-variations. In recent years serious doubts arose about the correctness of using a classical theory of atmospheric dynamo to explain these variations. Instead of neutral ionospheric winds as the main cause of S_q, Maeda (1966), Matsushita (1971), Lyatsky and Maltsev (1975) advanced independently and on different bases a hypothesis of magnetospheric dynamo which generates S_q^P- and S_q-currents simultaneously. In Glushakov and Samokhin's model (1974) a twin-vortex convection system in the outer magnetosphere generates not only the ionospheric S_q-system but also the main portion of the neutral wind field in the dynamo midlatitude ionospheric region.

In the event these hypotheses are true, the changes of S_q^P with B_Z should correspond to analogous changes of midlatitude vortices of S_q-currents. Figure 7

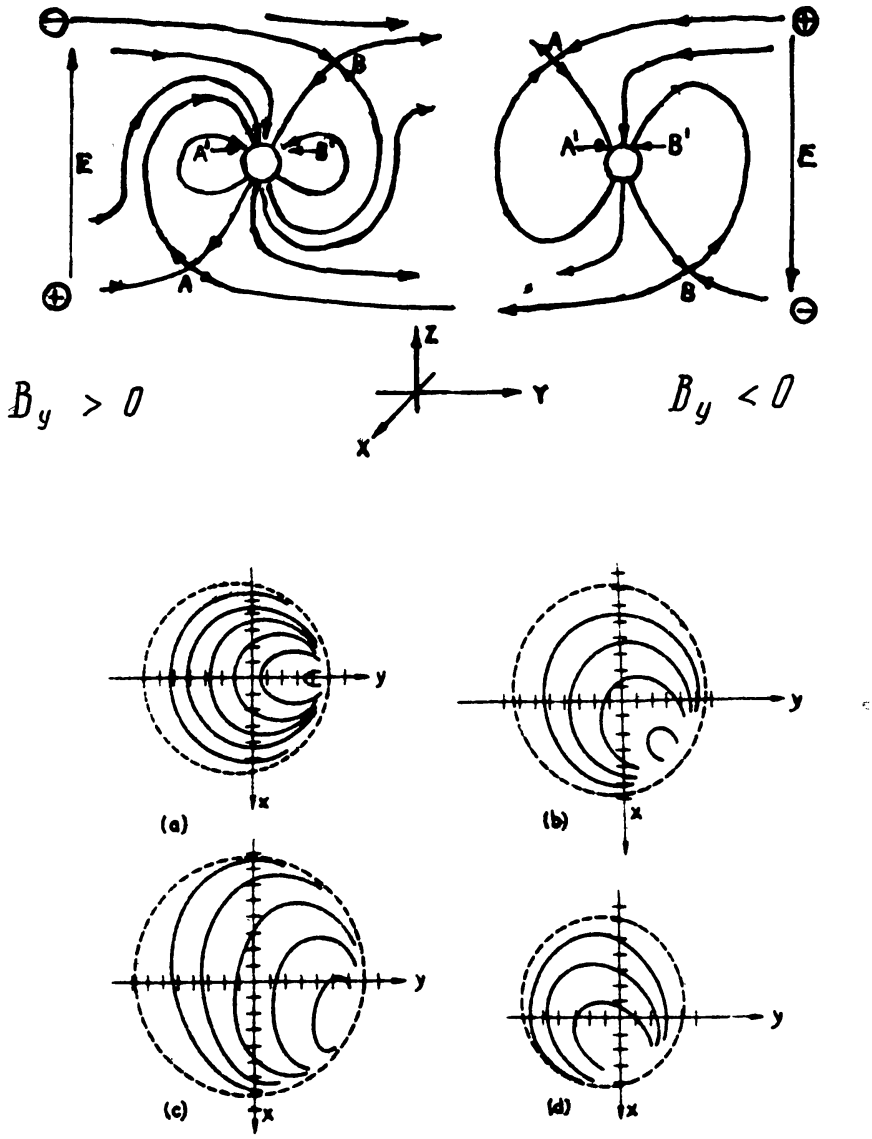

Fig. 6. Reconnection model after Stern (1973) (view from the Sun). Actual plot of equipotentials at intervals of 10^5 volts across the northern polar cap, when the simple model and an interplanetary electric field of 10^4 v/R_E are assumed. Axes meet at the pole and are marked at 2° intervals, whereas the polar cap boundary is marked by dashed lines. With the dipole field at the pole normalized to unity the drawings represent the following cases: (a) External field of 5×10^{-5} in the y-direction. (b) Component of 5×10^{-5} added to (a) in the direction antiparallel to x-axis, giving typical field of 'away' sector. (c) Southward component of 5×10^{-5} added to (b). (d) Northward component of 5×10^{-5} added to (b).

shows, however, that this consequence of the above hypothesis is not confirmed. A similar conclusion can be drawn from the comparison of S_q- and S-fields on data by Malin and Palumbo (1975) (see also Möhlmann and Wagner 1970). Hence, S_q^P and S_q have different causes and one ought to consider, as before, a dynamo-mechanism put into operation by neutral ionospheric winds of tidal origin as the main source of midlatitude (dayside) S_q-variations.

At the same time Figure 7 illustrates that sources of S_q^P contribute to the midlatitude S_q-field, since with changes of B_Z there occur slight but significant

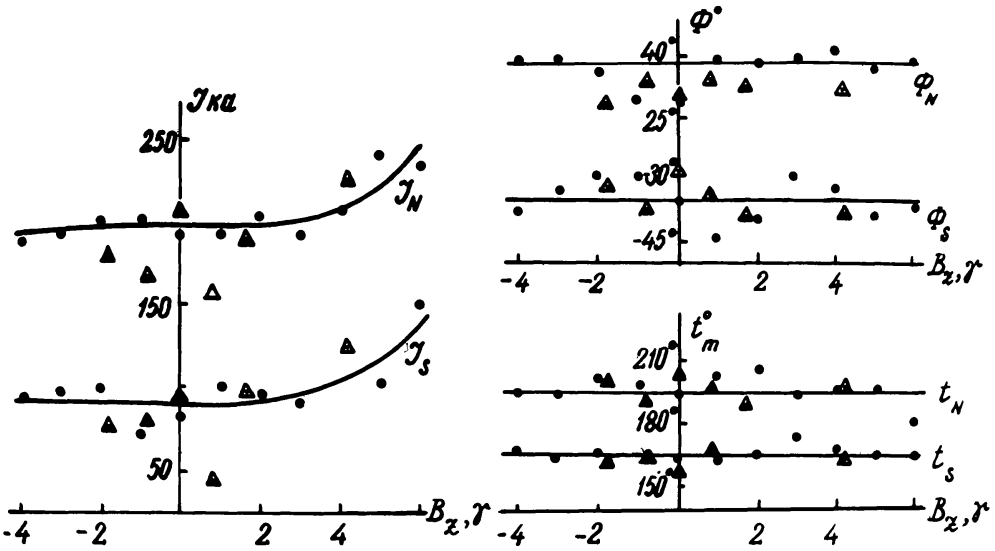

Fig. 7. Parameters of midlatitude S_q-vortices as a function of IMF B_z; T_N, T_S – values of a total current in the northern and southern S_q-vortices; t_N, t_S – latitude of foci, t_N, t_S – their local time. Dots – hourly, triangles – daily mean values.

variations of S_q-currents along with strong fluctuations of S_q^P-parameters. Such changes of S_q-field are most evident in the equatorial electrojet region (Nishida 1971; Beljakova *et al.* 1968; Matsushita and Balsley 1972). Our additional analysis has also shown that with increasing B_S harmonics V_1^0, V_1^1, and V_2^1 increase in the potential of the S_q-field that corresponds to intensity growth in the westward equatorial ring currents *DR* and DRP by 10–20%.

3.1.3. When comparing the equivalent S_q^P-currents and the 'dawn-to-dusk' electric field, we ignored the fact of the departure of current direction across the pole to the midnoon–midnight meridian and of the predominance of the dusk vortex of S_q^P-currents over the dawn one (see Figure 2). These irregularities are caused, evidently, by the fact that equivalent currents reflect the ground magnetic field not only of Hall currents, as was proposed above, but of two other portions of a three-dimensional system in Figure 3b as well – the Pedersen and field-aligned currents. These two portions correspond to equivalent currents, directed in the polar cap from dawn to dusk (T_1) and vice versa (T_2). Due to the fact that electroconductivity of the polar ionosphere at the dayside is greater than at the nightside, inequalities take place: $T_1 > T_2$ for the dayside, and $T_2 < T_1$ for the nightside.

So, the day–night asymmetry in distribution of ionospheric electroconductivity ensures that the contribution of the current system $T_1 + T_2$, directed eastward throughout, is superposed onto the contribution to the equivalent currents produced by Hall currents. Superposition of such a quasi-zonal eastward current onto a double-vortex system yields in the latter the predominance of the dusk vortex, as shown in Figure 8.

The second important cause of asymmetry in electroconductivity distribution is an auroral zone at $\Phi = 65$–$70°$. In this zone the ionospheric conductivity experi-

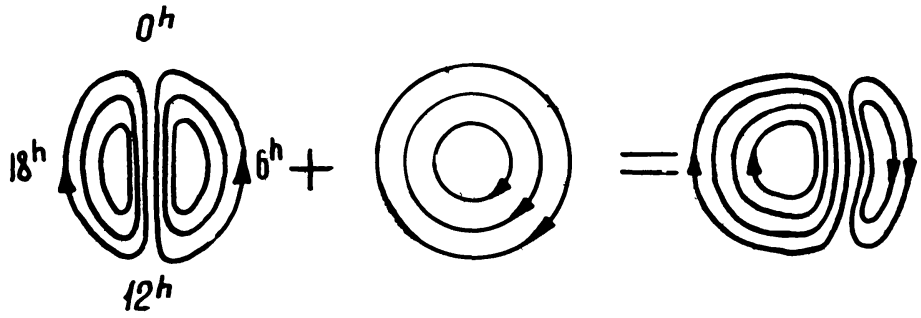

Fig. 8. A schematic illustration of superposition of zonal convection onto the two-vortex one in the polar cap.

ences an appreciable increase, resulting in attenuation of the Pedersen current across the polar cap, compared with a case of uniform ionosphere. Eventually, a contribution of field-aligned currents to the ground magnetic field perturbations measured in the polar caps appears to be predominant over that of Pedersen currents, i.e. the sunward Hall current is superposed with the equivalent one, directed from dusk to dawn. The resulting polar cap current turns out to be deflected clockwise from the midnoon–midnight meridian. Lyatsky and Maltsev (1975) have shown that such an interpretation can perfectly stand up to a quantitative check.

In conclusion we would like to note that the equivalent systems in Figure 1 are calculated with the diurnal mean reference level of S_q-variations, since the real reference level is unknown. Mishin *et al.* (1971) presented the analysis of S_q^P-fields, reckoned from the level of night hours. The currents, equivalent to a magnetic field of the difference between two reference levels, are shown in Figure 9 (on data by Bazarzhapov *et al.* 1971). One can see strong changes in the configuration of these currents, caused by daily motions of the geomagnetic polar cap with respect to the sunlit geographic polar cap.

This also means that different factors, like B_Z, B_Y and solar wind velocity (Murayama and Hakamada 1975), produce fluctuations in S_q^P, i.e. fields

$$\delta = S_q - \bar{S}_q$$

which turn out to be compatible in strength with the mean S_q^P-field and contain useful information. As shown by Kane (1971), the traces of δ-fields produced by Z, Y and/or X components of the IMF are also noticeable in the S_q-field of middle and low latitudes (see also Figure 7). Therefore we shall proceed with a consideration of δ-fields. The subsequent section of this paper deals with description of δ-currents, generated in high latitudes by meridional electric fields which occur like the 'dawn-to-dusk' field as a result of fluctuations in the Y-component of the IMF.

3.2. δ_Y-FIELDS

Large-scale magnetic fields in the solar environment form the so-called sectors or portions of the field with typical dimensions in longitude $2\pi/4$ (7 days). The

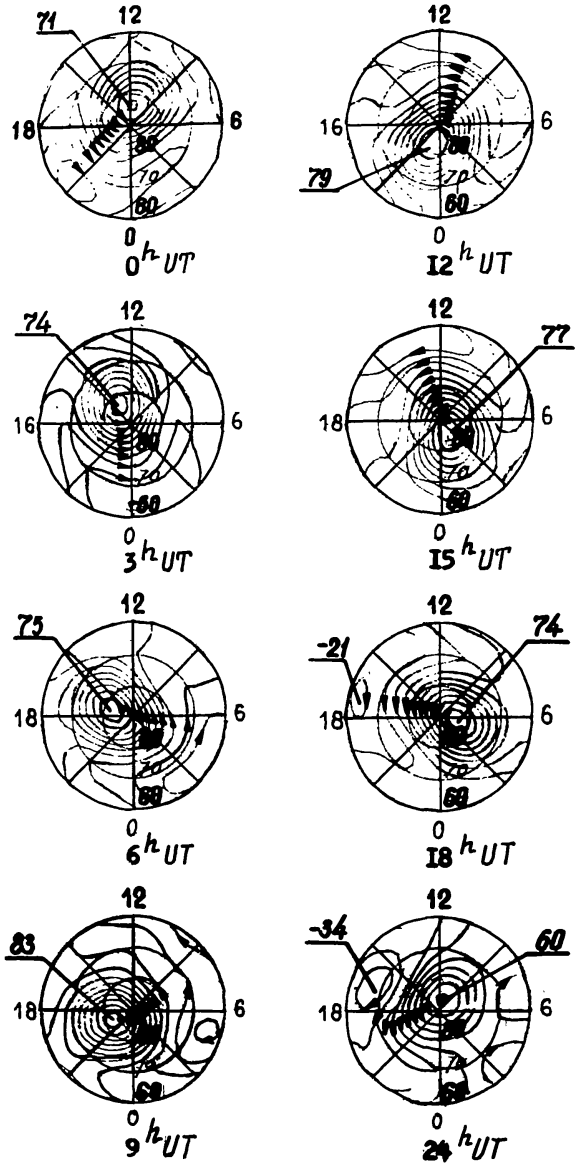

Fig. 9. Currents, equivalent to the difference of magnetic fields – diurnal mean and night (quiet days). Focal values – in kiloamperes, coordinates – geomagnetic latitude and geomagnetic time.

magnetic field lines inside each sector are extended in the ecliptic plane along Archimedian spirals, twisted with respect to solar rotation. The ecliptic components along axes X (sunward) and Y ('dawn–dusk') have a value of several gammas and the signs, depending on the sector sign. In the 'away' sector $B_X < O$, $B_Y > O$. Z-component of the IMF is produced by 'crimping' of the sector structure and has a comparatively small space scale, corresponding to preservation of sign B_z in the vicinity of the Earth over several hours.

Svalgaard (1968) and Mansurov (1969) have shown that at the dayside high-latitude region $\Phi > 75°$ there are specific geomagnetic variations, occasionally amounting to hundreds of gammas, whose form is determined by the IMF sector sign. Examples of such variations in days with a well-pronounced sector structure

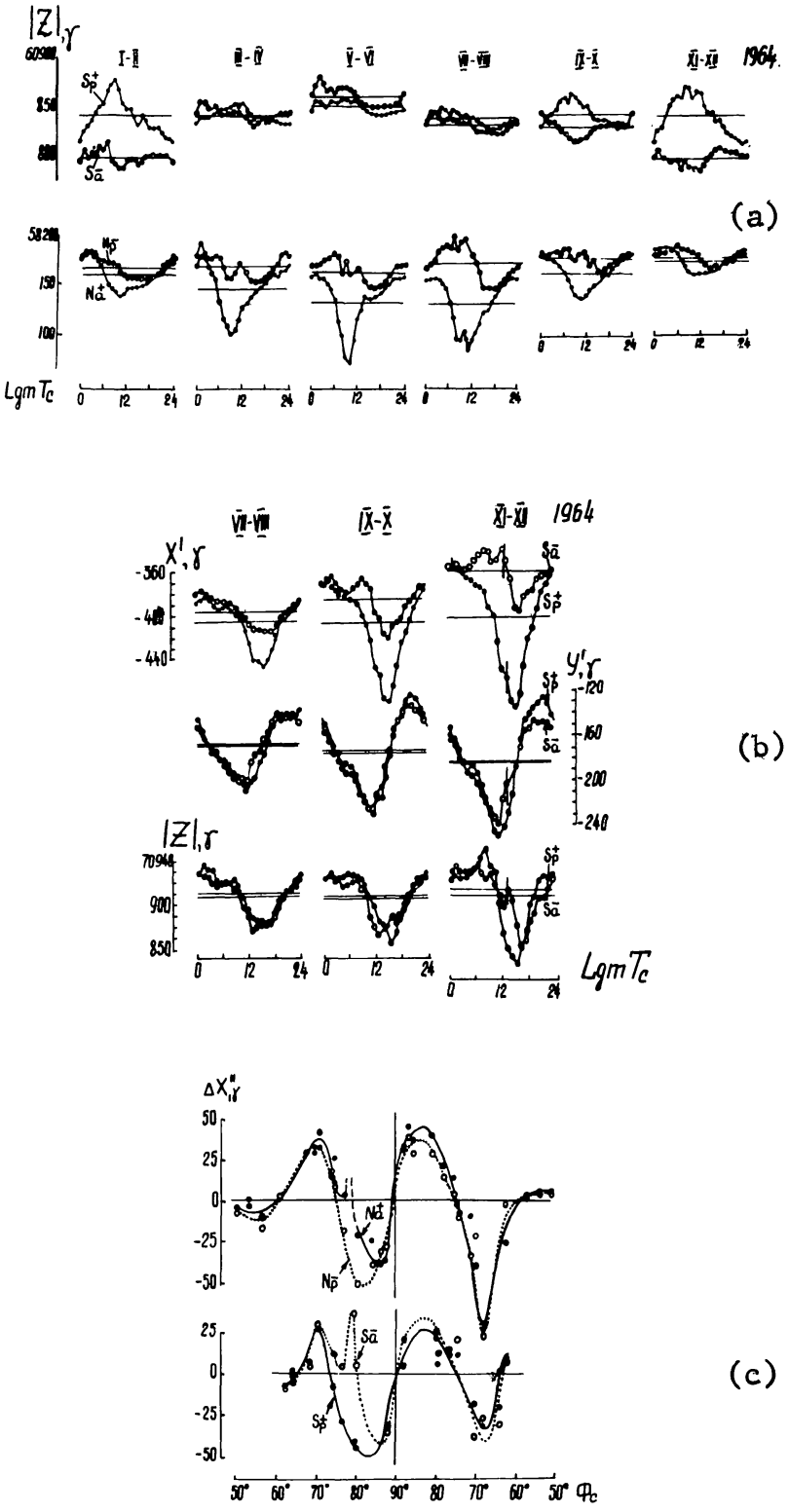

Fig. 10. Geomagnetic variations in polar caps for away (dots) and toward (circles) IMF sectors. (a) Annual changes of geomagnetic daily variations at Vostok (*S*) and Resolute Bay (*N*). (b) Daily variations at Dumont D'Urville (*S*). (c) Latitude profiles of the *X*-component along the 'midnoon-midnight' meridian for the northern (top) and southern (bottom) hemispheres, reckoned from the daily mean level (to the left – midnoon, to the right – midnight meridians of the local geomagnetic time LGMT), (after Bassolo *et al.*, 1972).

of the IMF are given in Figure 10. In the polar cap the IMF sector sign change is seen to be accompanied by a sharp variation of the ground magnetic field in the pre-noon hours, so that during this period variations $\delta = 0.5\ (S_q^+ - S_q^-)$ take place whose range in the X-component is maximum at about $\Phi = 80°$. With increasing latitude at $\Phi > 80°$ the relation $\delta Z/\delta X$ increases as well. δY-variations are less than δX and δZ,

These facts demonstrate that quasi-zonal currents, flowing mainly near $\Phi \approx 80°$ at the daytime, should be a source of δ-variations of the type described above. In order to be consistent with the data in Figure 10, these currents should be eastward in the northern hemisphere and westward in the southern one for the away IMF sector and vice versa for the toward sector. Later, in works by Friis–Cristensen *et al.* (1972) and some others (Shelomentsev 1974; Mishin *et al.* 1975*b*; Sumaruk and Feldstein 1973) such variations were found to be caused completely by fluctuations of the IMF Y-component, i.e. B_X-field is practically unessential. Therefore, we shall label below such variations by the symbol δ_Y.

A general system of currents, equivalent to a high-latitude δ_Y-field, is obtained by Mishin *et al.* (1975b), where the data of the world-wide network of magnetic stations at $\Phi \geqslant 60°$ and the method of analysis described in § 1 where used. Figure 11 illustrates δ_Y-currents for V-VIII, 1958. It is seen, as predicted, that the basic element of the system at daytime is the quasi-zonal currents whose direction depends on B_Y-sign and is different in two hemispheres. Figure 12 shows that the direction of δ_Y-currents even at daytime is close to a zonal one only in the daily mean pattern and at the selected UT-moments when the geomagnetic polar cap is entirely sunlit. At other UT-hours the direction of δ_Y-currents differs appreciably from the zonal one.

These data point also to the existence of rather strong UT-variations of intensity of δ_Y-currents, having, evidently, the same nature as UT-variations of S_q^P-currents, controlled by illumination conditions of the geomagnetic polar cap (see also Figure 9 and the work by Feldstein *et al.* (1974)).

Note that δ_Y-currents in Figure 11 are observed both at day and night sides and the region of their density maximum is a closed circular zone near $\Phi = 76$–$80°$ *where the polar electrojet is flowing.* This zone apparently corresponds to a projection of the so-called cleft into the geomagnetosphere – a main channel through which thermalized solar wind plasma is injected into the magnetosphere. Such a conclusion is not contradictory to Fairfield and Mead's magnetosphere model (1975) (Figure 13) and corresponds to Stern's model in which the polar cap boundary is a closed quasi-circle at $\Phi = 76$–$80°$ (Figure 6).

Jørgensen *et al.* (1972) were the first to assume that the high-latitude δ_Y-currents are produced by the transfer of the potential of solar wind electric field $-\mathbf{V} \times \mathbf{B}_Y$ along geomagnetic field lines into the magnetosphere as a consequence of magnetopause reconnection between IMF and a geomagnetic field. Projections of field $-\mathbf{V} \times \mathbf{B}_Y$ onto the polar ionosphere are obtained in works by Stern (1973), Matveev and Mishin (1975), Leontjev and Lyatsky (1974). Stern's results are

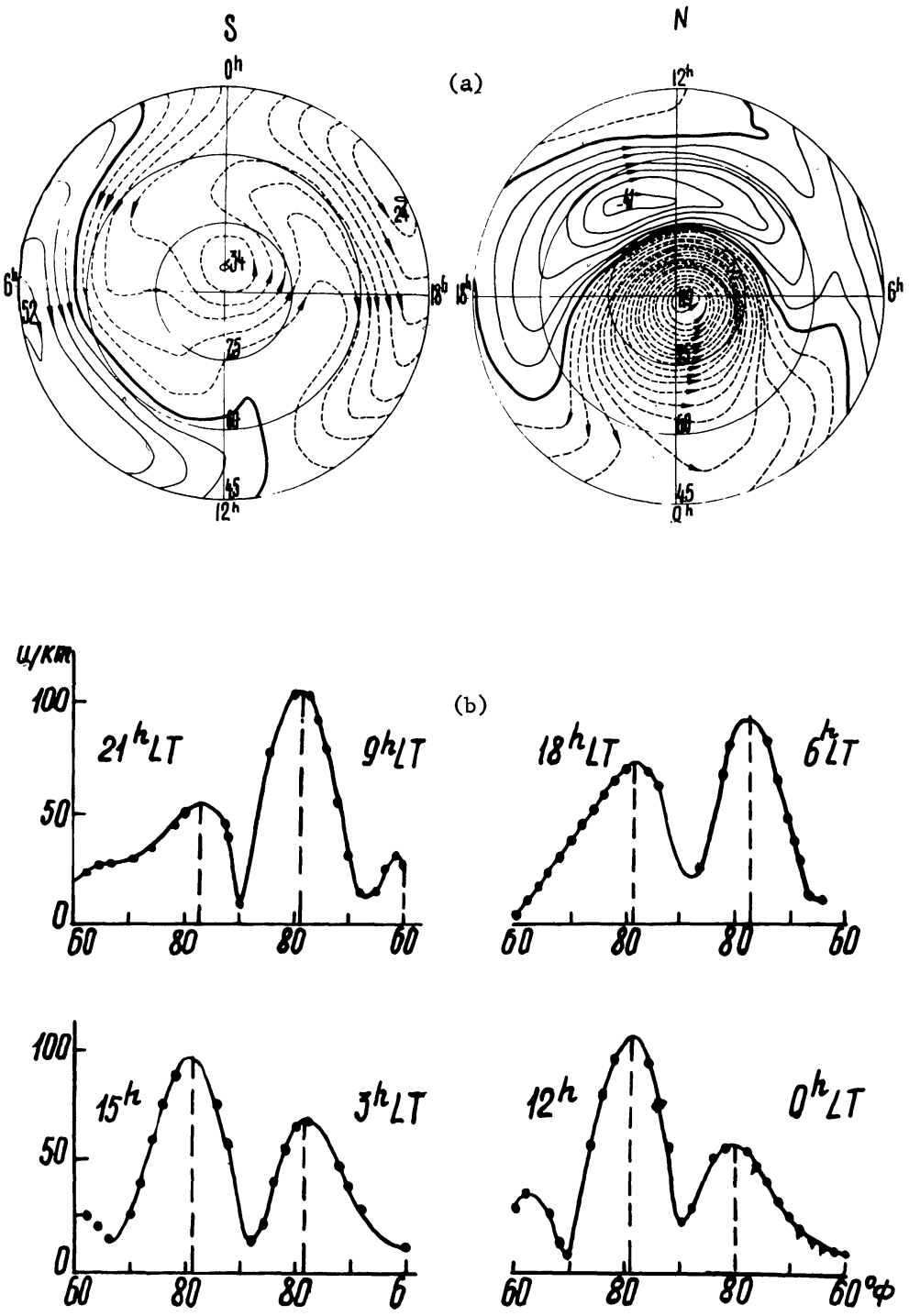

Fig. 11. *Top:* equivalent δ-currents on data of V-VIII, 1958. Focal values – in kiloamperes; coordinates – geomagnetic latitude and time. *Bottom:* latitude variations of j (module of density of δ-currents) along the four LT-meridians. A zone of maximum j is seen to have a quasi-circular shape (Mishin *et al.*, 1975a).

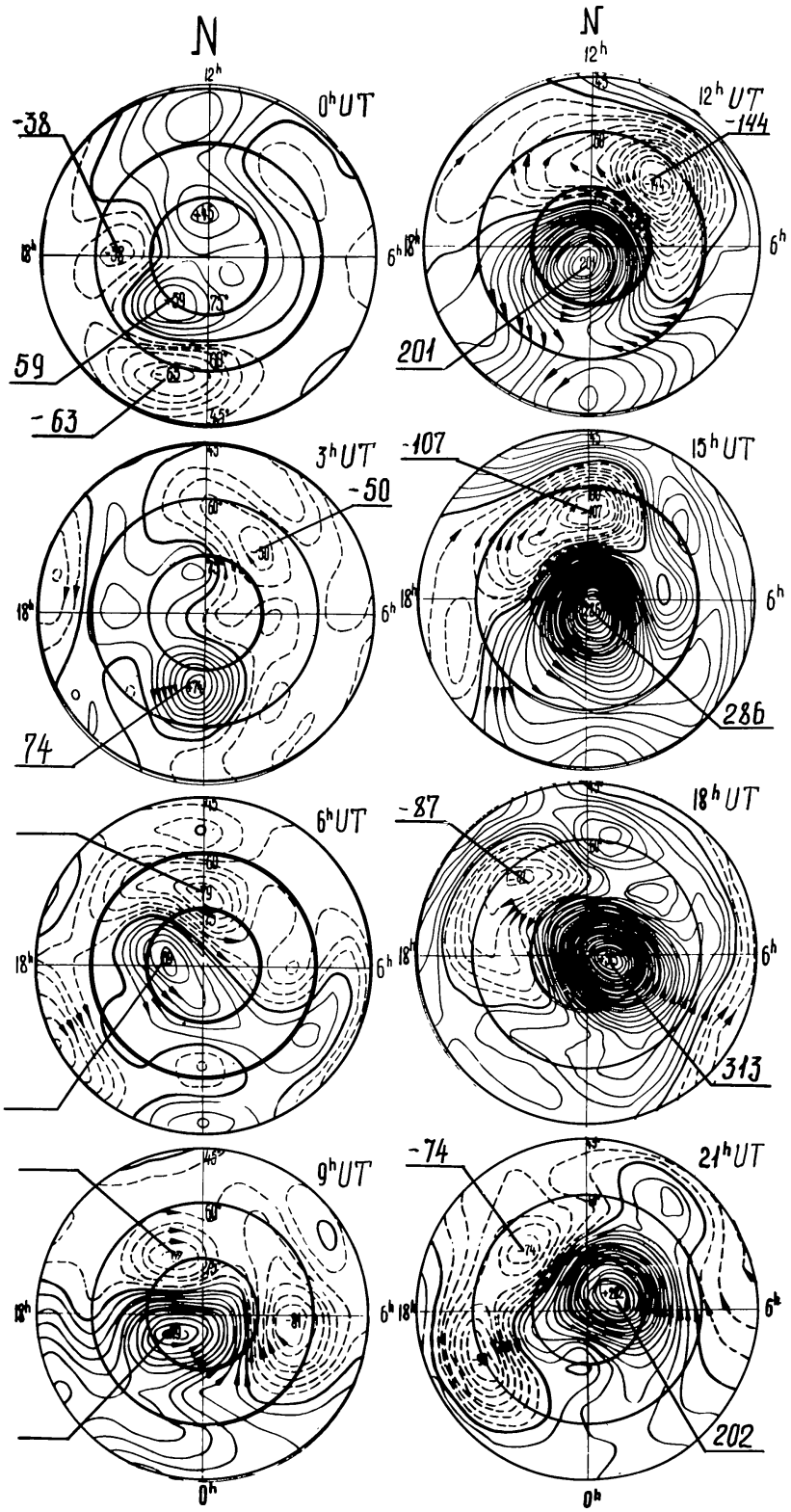

Fig. 12. Systems of δ_y-currents at different UT-hours (V-VIII, 1958). Coordinates – geomagnetic latitude and time, focal values – in kiloamperes. The enhancement of zonal corrents is seen in the sunlit geographic polar cap which is moving with UT relative to a geomagnetic pole.

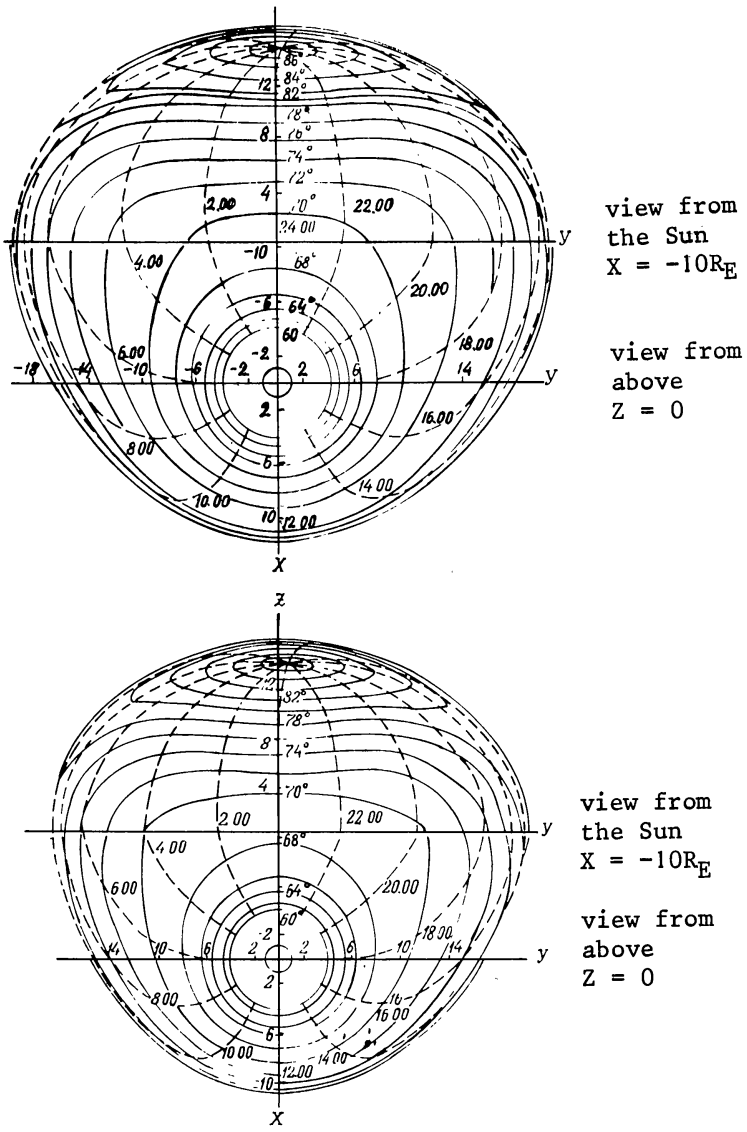

Fig. 13. A geomagnetosphere model by Fairfield and Mead (1975). Contours of constant latitude (solid lines) and constant local time (dashed lines) at the Earth's surface as mapped along field lines of the MF73Q field model ($K_P < 2$) to the equatorial plane (bottom) and to a tail cross section at $X = -10R_E$ (top). The dipole tilt angle is zero. (a): $K_P < 2$, (b): $K_P > 2$.

presented in Figure 6. Field $-\mathbf{V} \times \mathbf{B}_Y$ is northward (in the solar-ecliptic system) at $B_Y > 0$ (an away IMF sector) and is southward at $B_Y < 0$. A projection of this field onto the polar ionosphere, corresponding to the magnetosphere model by Fairfield and Mead (1975), is shown in Figure 14. A basic portion of the ionospheric electric field is seen to have a meridional direction. A combination of such a field with the 'dawn-to-dusk' one yields the 'dawn–dusk' inequalities in the latter, as shown in Figure 15. These results agree with Heppner's measurements (1972).

The electric field in Figure 14, with the given ionospheric electroconductivity model being approximate to the empirical one by Vanjan and Osipova (1973), corresponds to a three-dimensional system of currents, shown in Figure 16 as a

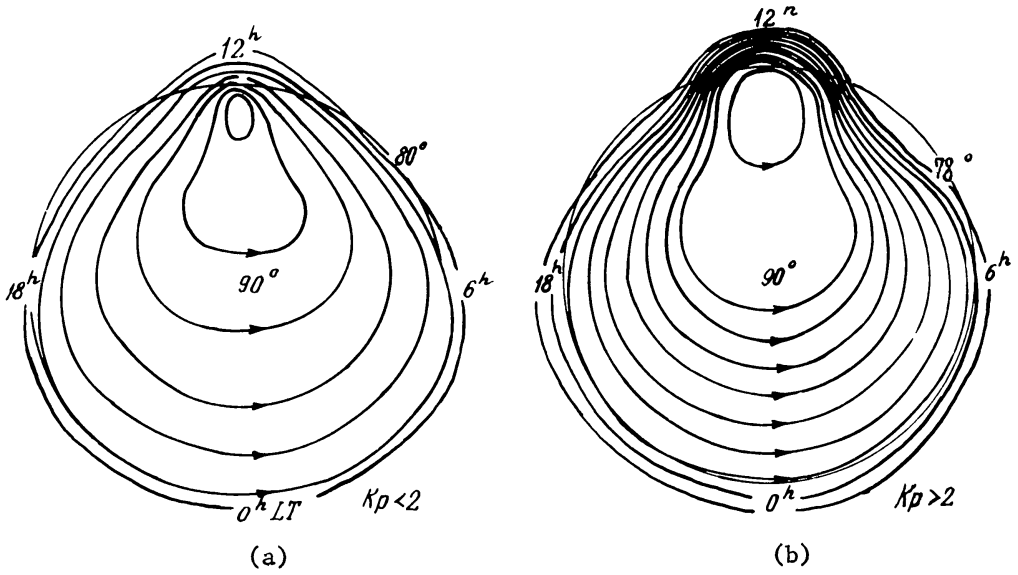

Fig. 14. Equipotentials of the E_Z (Z-component of the electric field $-\mathbf{V}\times\mathbf{B}_2$, obtained by mapping along magnetic field lines onto the northern polar cap) (see caption to Figure 5b). You can see the maximum of meridional field E_z near $\Phi\approx 80°$ at all LT-hours (Matveev and Mishin 1975).

projection onto the midnoon–midnight meridian (for the away IMF sector). The heavy arrow in this figure is a Hall polar electrojet, dotted lines are Pedersen currents, and solid ones some of field-aligned magnetospheric currents. According to Matveev's estimations (1974) the intensity of the Hall polar electrojet for $B_Y = 3\gamma$ and for summer conditions is 100 kA, the intensity of field-aligned currents bordering the polar electrojet with two 'curtains' from north and south is $\approx 1.5\times 10^6$ Amp. A main contribution to the high-latitude ground magnetic field is made by Hall currents, and a two-dimensional system, equivalent to a three-dimensional one shown in Figure 16, is close to the observed one (Figure 11). The existence of field-aligned currents (Figure 16) in the form of two 'curtains' is confirmed by satellite magnetic measurements (Armstrong and Zmuda 1970).

3.3. Midlatitude Δ_Y-fields

In works by Aksenova *et al.* (1971), Mishin and Aksenova (1974), and Mishin *et al.* (1975c), specific geomagnetic variations whose form depends on IMF sector

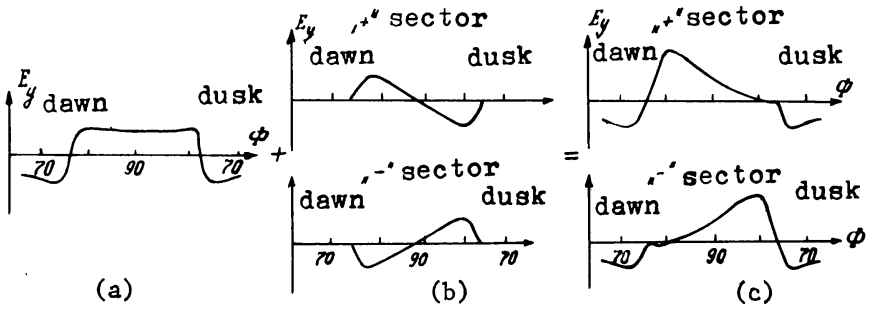

Fig. 15. Superposition of electric fields: 'dawn–dusk' (a) and meridional (b) for the away and toward IMF sectors.

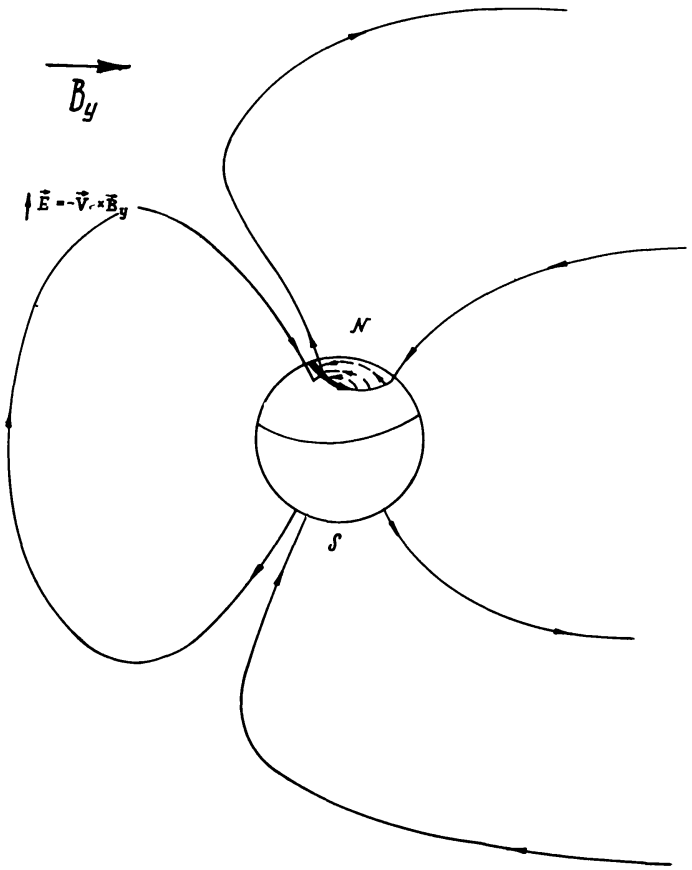

Fig. 16. A scheme of three-dimensional current system, caused by Z-component of the tail electric field $-\mathbf{V}\times\mathbf{B}y$. Field-aligned currents, a Hall polar electrojet (a heavy arrow near $\Phi = 78°$) and a portion of Pedersen currents (dotted lines) are shown. A similar system in the southern hemisphere is not illustrated.

sign are shown to take place both in middle and low latitudes* . Examples of such variations, labelled below by the symbol Δ_Y, are given in Figure 17. They are defined as differences $X = X - \bar{X}$, $Y = Y - \bar{Y}$, $Z = Z - \bar{Z}$ where X,Y,Z are instantaneous values and $\bar{X},\bar{Y},\bar{Z}$ mean ones taken over a great number of quiet days, involving equally both IMF sectors. One can see in Figures 17 and 18 that Δ-variations of X and Y components experience a phase shift: in the away IMF sector ΔY amounts to a maximum value at about midnoon at all latitudes of both hemispheres, whereas ΔX passes across zero at this moment. The phase of the diurnal variation X changes to the opposite one near the equator. The above-described latitude distribution of Δ-variations is shown in Figure 18a.

Assuming $\mathbf{j} \sim \Delta\mathbf{H}\times\mathbf{n}$, where $\Delta H = \sqrt{(\Delta X)^2 + (\Delta Y)^2}$, j is a surface current density, $\mathbf{n}$ is an outward normal to the Earth's surface, it is easy to construct a two-dimensional system of the surface currents equivalent to Δ_Y-field. It is evident that in the pre-noon region Δ_Y-currents are directed along the meridian: southward and northward in the away and toward IMF sectors, respectively. The

* When averaging the data of a great number of quiet days, the contribution of such variations is eliminated since they are opposite in two IMF sectors.

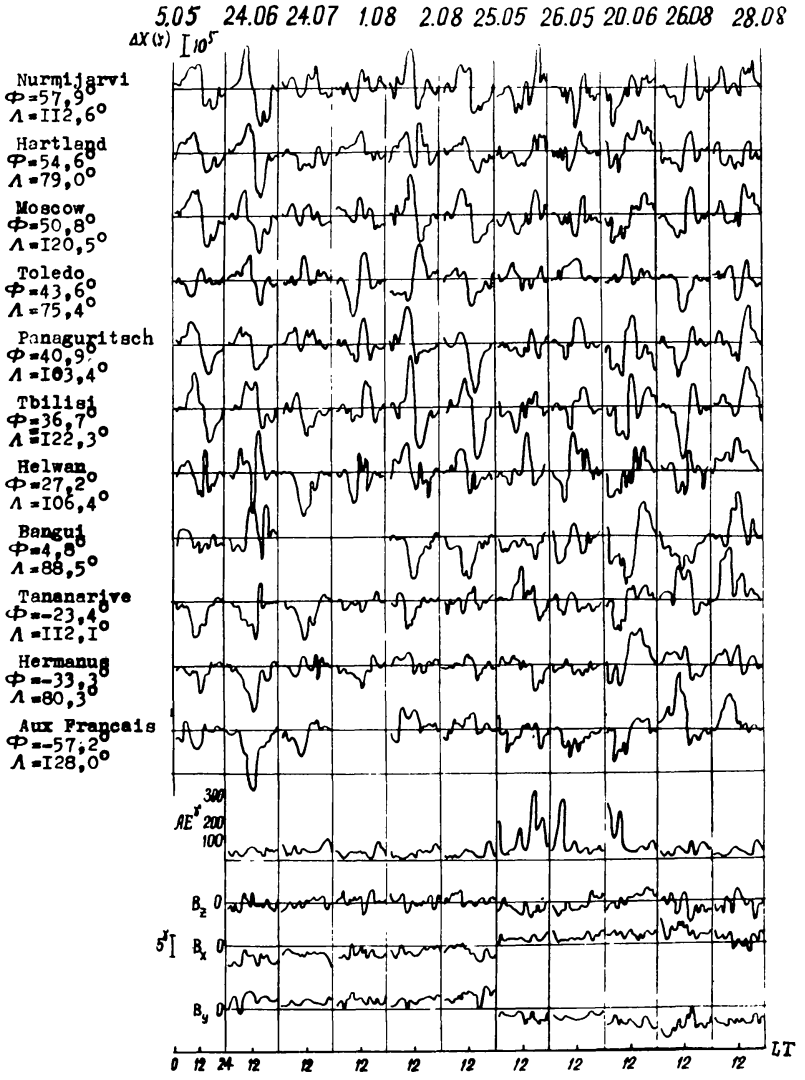

(a)

Fig. 17. Variations $\Delta = S_q^{P+} - S_q^{P-}$ on data of V-VIII, 1958. The 1st column – averages over 10 days, further – data of individual days, listed at the upper line. *Below:* indices AE and values of IMF (reproduced by courtesy of Dr A. Nishida). Abscissae – local time at meridian $\lambda = 100°$.

(a) $-\Delta X$, (b) $-\Delta Y$, (c) $-\Delta Z$.

closing currents consist of two vortices with the foci near the equator – a negative (clockwise) vortex in the dawn sector and a positive one in the dusk sector, as shown in Figure 18b. In the toward IMF sector Δ-vortices alter their signs.

Density and value of the meridional current near the midnoon are defined by the range of diurnal variation Y in Figure 18 and by the width of the current sheet, which can be estimated by the distance between coordinates t_1 and t_2 of the maximum and minimum ΔX.

This results in a total current ~100–150 kA and the intensity of each vortex is 50–70 kA*.

* ΔH (gammas) $\approx j$ a km^{-1}.

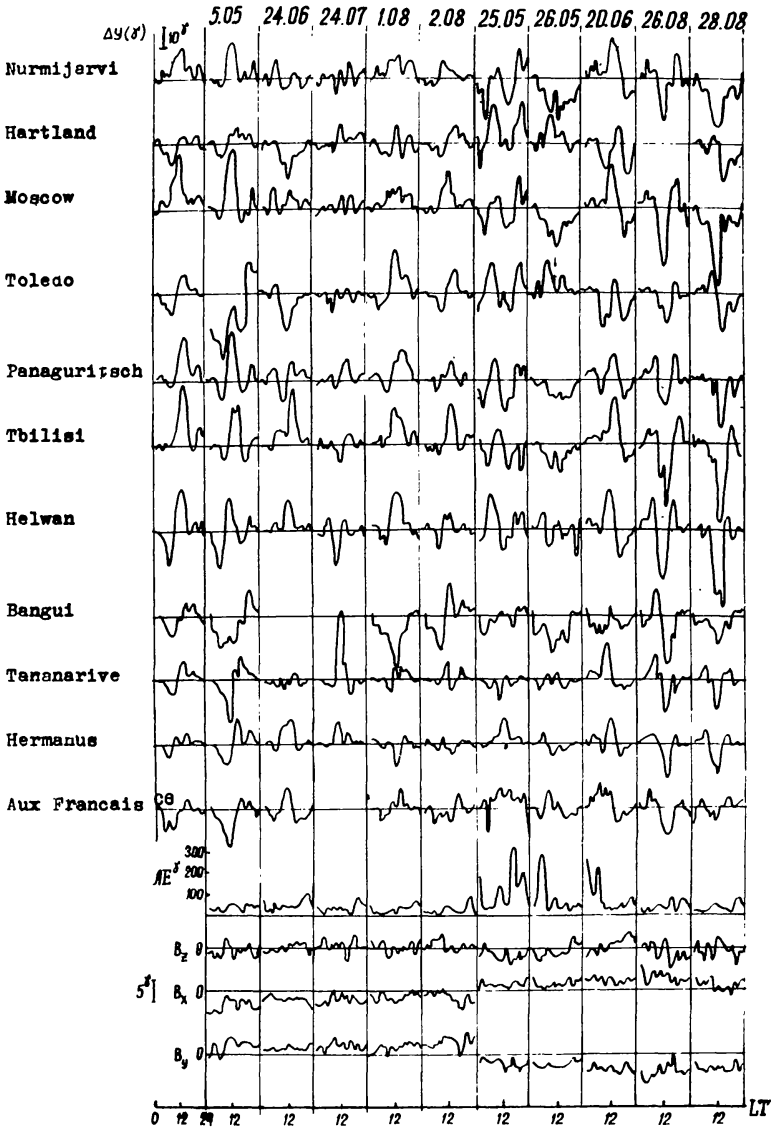

(b)

Fig. 17 (*cont'd*).

Examples of two-dimensional equivalent Δ-currents, obtained by hourly data of selected quiet days, are shown in Figure 19. One can see that these data agree with the picture given above. Calculation of the potential of Δ-fields enables us to outline some additional significant features.

In the potential of Δ-field, as opposed to the S_q-one, the basic is an even harmonic V_1^1, followed subsequently (according to the contribution to the potential) by harmonics V_2^2 and V_1^0. Harmonics V_1^1 just determine the main features of Δ-field noted above – they are consistent with a two-vortex system of currents with foci at the equator. Harmonic V_2^2 produces the asymmetry of main vortices and may increase their number, whereas due to harmonic V_1^0 the foci are shifted from the equator. Both these features are shown in Figure 18b. One can see also that two main vortices are unequal in intensity; a dawn vortex is predominant. This allows a simple interpretation, which will be given below. Preliminarily, we note the following.

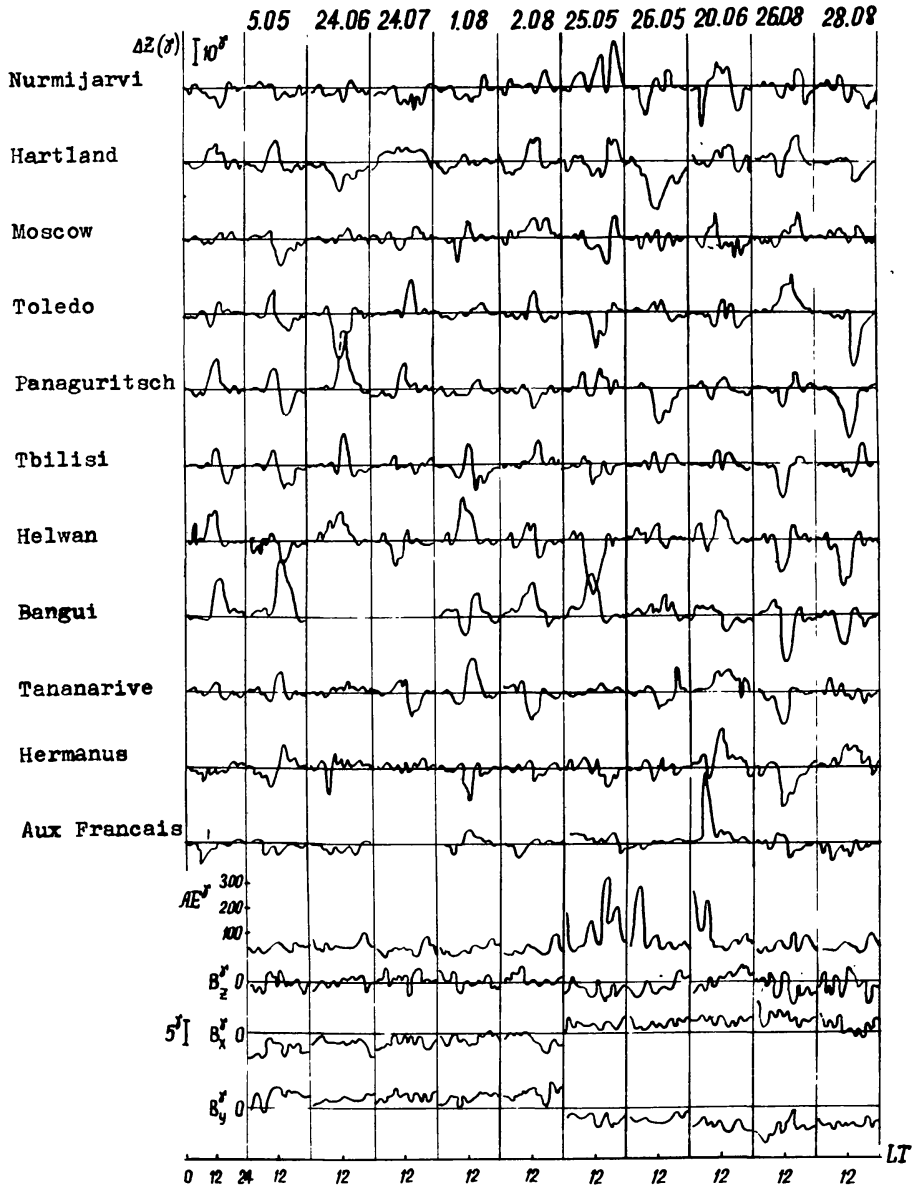

(c)

Fig. 17 (*cont'd*).

Mishin *et al.* (1975c) have shown by comparison of Δ-variations with fluctuations of X- and Y-components of the IMF that these variations are produced by IMF B_Y like the high-latitude δ_Y-ones. This can be seen in Figure 17. Indeed, for selected days given in this Figure, $B_X \to 0$ does not influence the characteristics of Δ-variations.

So, the midlatitude Δ-variations have the same cause as the high-latitude δ_Y-field and their source should be a three-dimensional system of currents δ_Y. To show it, Figure 20 schematically presents the basic elements of a three-dimensional δ_Y-system (they are inferred from Figure 14) and the corresponding two-dimensional equivalent currents.

The basic harmonics of a current function and their amplitudes are noted, corresponding to case $B_Y \approx 5\gamma$, when the Hall polar electrojet is eastward and westward in the N- and S- hemispheres, respectively, with intensity 150 kA. Let

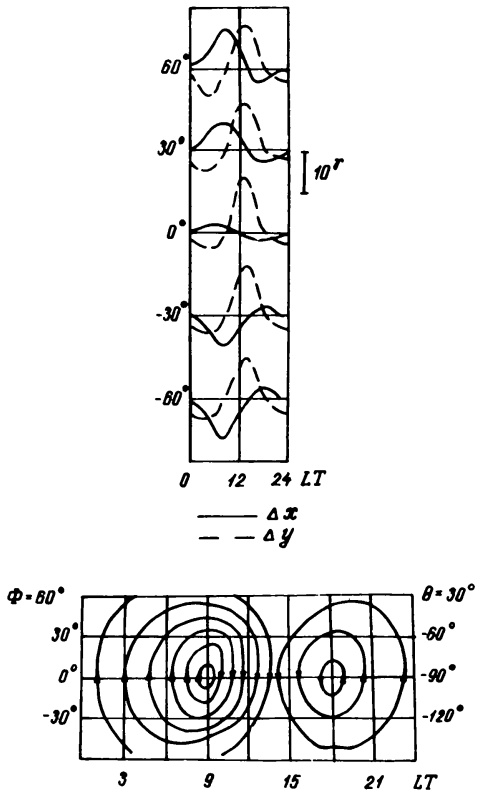

Fig. 18. A model of midlatitude Δ-variations (a) and of equivalent systems of Δ-currents (b).

us explain this pattern in terms of the first contour of Figure 20. In this case a magnetic field in middle latitudes is produced by two pairs of field-aligned currents, each being located to the north or to the south of the measurement points at greater distances, as compared with the source dimensions. Such a magnetic field, like the field near the solenoid axis, is close to a homogeneous one and is directed (for the case of Figure 20a) outside the drawing plane. It is described by the scalar potential, involving only one harmonic P_1^1 (cos θ) cos t.

Thus, a three-dimensional model of δ_Y-currents describes ground magnetic fields produced by them both in high and middle latitudes.* Consequently the latter are one more feature of the reconnection process between IMF and the geomagnetic field, supporting a fundamental role of this process in production of electric fields and currents in the geomagnetosphere.

4. Magnetic Substorms and Disturbances in the Magnetosphere

4.1. Magnetospheric substorms

4.1.1. *Introduction*

Magnetospheric substorms – the main type of magnetospheric disturbances – are produced by interplanetary shock waves during solar flares or are caused by the

* In the latter case one ought to take into account additionally harmonic T_1^0, whose origin is not clear as yet.

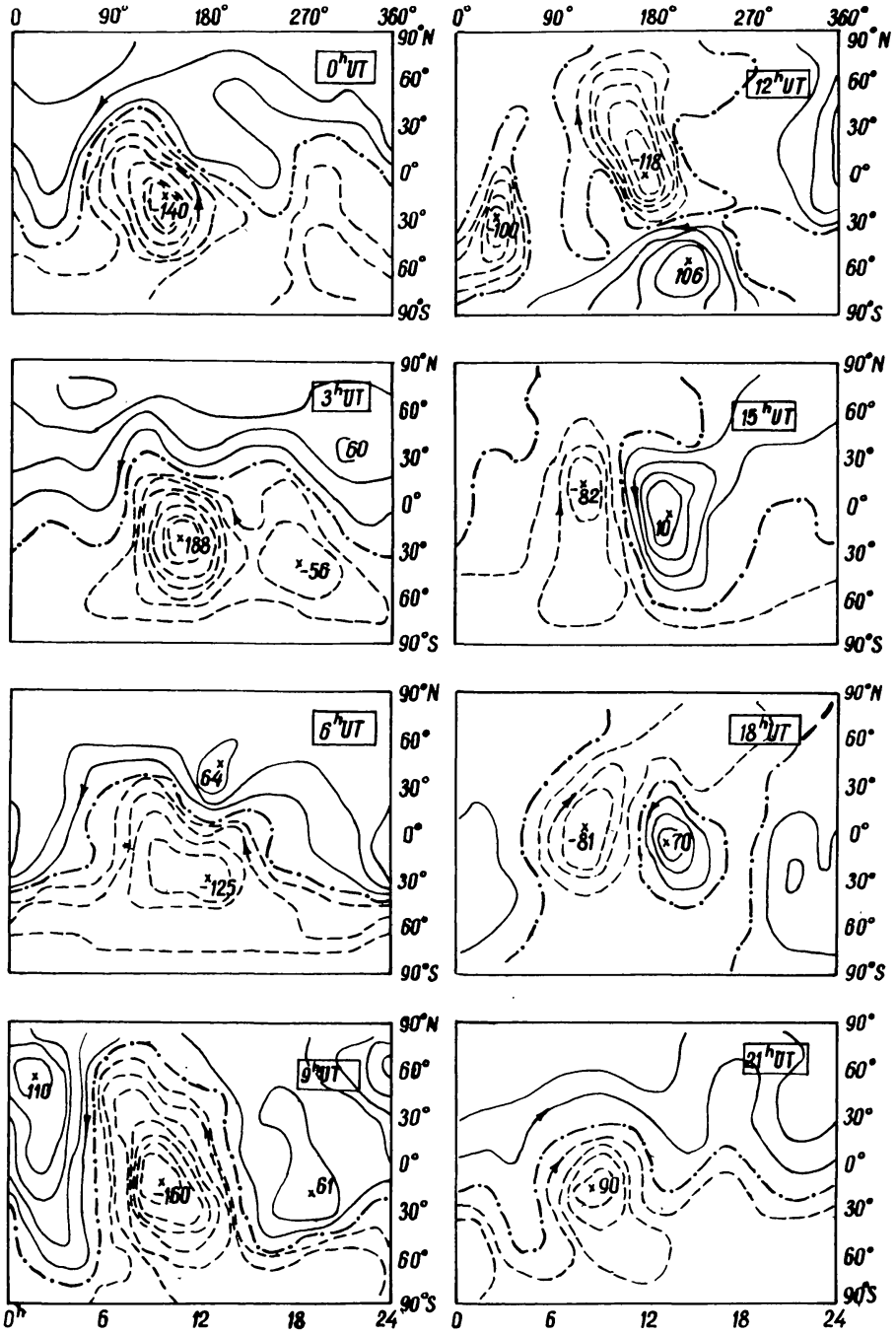

Fig. 19. Equivalent systems of Δ-currents on data of January 7, 1958 (an away IMF sector) (Aksenova *et al.*, 1971).

appearance of the IMF in the near-Earth environment with a great enough south component. Below some other possible causes of substorms will be noted. Typical duration of substorms is several hours, and the characteristic energy 10^{22}erg. Substorms occur either as isolated events with intervals $\geqslant$12 hr or as a successive superposition of isolated events thus resulting in a magnetospheric storm.

Modern representations of substorms have been developed over the last 15 years, beginning with works by Dungey (1961), Axford and Hines (1961),

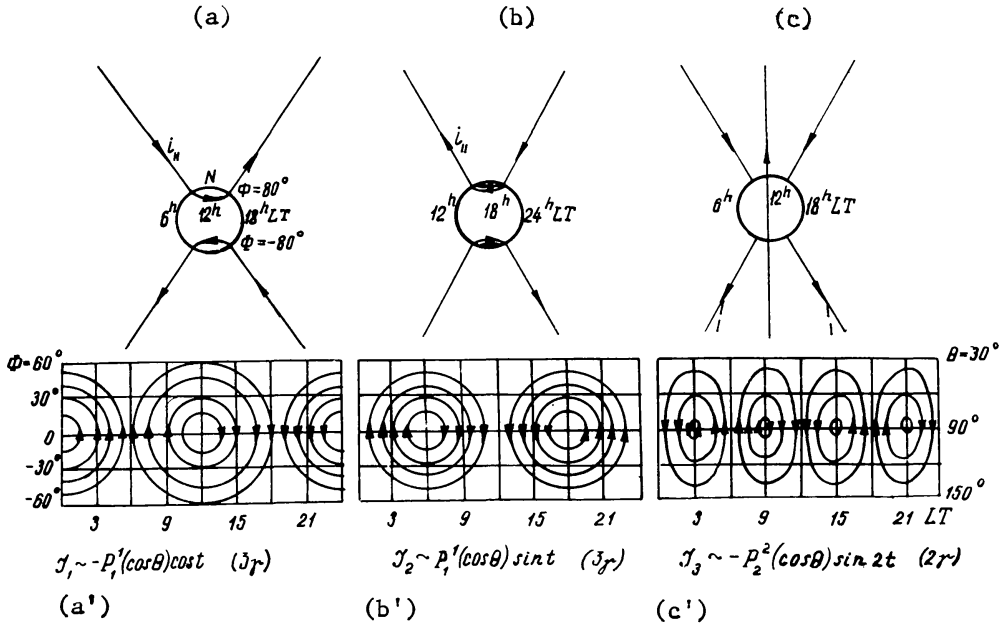

Fig. 20. A Scheme of three main elements of a three-dimensional system of magentospheric δ-currents, caused by Z-component of electric field $-\mathbf{V}\times\mathbf{B}_y$ (*a*, *b*, *c*) and their approximate two-dimensional equivalents in middle and low latitudes (*a'*, *b'*, *c'*). *Bottom:* main harmonics of a current function and their amplitudes in gammas.

Piddington (1964) and even earlier (Birkeland 1908), though the first statements on substorm concepts as well as the notion itself emerged only later (Coroniti *et al.*, 1968; Akasofu 1968). Many attempts have been made by a number of research workers to develop the existing concept; the most complete, but by no means comprehensive, bibliography is given in the monograph by Akasofu and Chapman (1972), in reviews by Roederer (1974), Siscoe (1975), Crooker (1975), Rostoker (1975). This concept involves a phenomenological substorm model and the elements of its theory which, eventually, permit understanding semi-qualitatively the fundamental processes but still contain some controversies.

There is no doubt that the substorm energy is transferred to the magnetosphere from the solar wind, but the mechanisms of the energy, momentum and mass transfer are not clear as yet. These mechanisms depend, certainly, on the IMF, thus indicating the important role of the magnetopause reconnection process. In particular, it is well stated (see reviews by Burch 1974, Nishida 1975, Akasofu 1975a,b) that at $B_Z<0$ (South IMF) the substorm intensity enhances and their main activity zone ('auroral oval') expands, compared with the case $B_Z>0$ (north IMF).

The most complete study was made of substorms caused by solar plasma streams with the south IMF. This is conditioned by the fact that at $B_Z<0$ the main jet currents of the substorms cover latitudes $\Phi=65$–$70°$ where a great number of magnetic and auroral stations are located, whereas at $B_Z>0$ basic ground substorm signatures shift to $\Phi>70°$ where there are few observatories (Akasofu *et al.*, 1973, Akasofu 1975a,b).

4.1.2. *Substorms at the South IMF*

A substorm of this type apparently consists of the following sequence of basic events.

After the southward turning of the IMF, the reconnection speed of solar wind magnetic fields and of a terrestrial one is increased.

Magnetic field lines of the dayside magnetopause are transported to the tail, increasing a magnetic flux and the main (two-vortex) magnetospheric convection system there. In the boundary magnetospheric layer the plasma moves in the anti-solar direction; in the inner portion of the tail the plasma sheet slows down the development of the return convection, therefore the latter develops here with a time lag 10–30 min that allows for the accumulation of magnetic energy in the tail. Due to the return convection, particles of a boundary transient layer are transported to the inner edge of the plasma sheet and are accelerated. The hot plasma occupies drift shells at $L = 6$–7 in the vicinity of the above-mentioned inner edge which was at $L = 8$–9 prior to the substorm. At the same time currents of the plasma sheet are enhanced and the stretching of the tail magnetic field lines is increased, ring currents DRP and DR also being enhanced.

Drift velocity of the plasma sheet ($\mathbf{E} \times \mathbf{B}$) has also a neutral layer directed component. Therefore, in the course of the above-described initial phase the plasma sheet is thinning and thus promoting the subsequent generation of neutral lines near the inner edge of the plasma sheet, i.e. the reconnection process. This is favored also by the enhancement of particle precipitation from the inner edge of the plasma sheet to the ionosphere of the auroral zone, which takes place during the initial phase. Indeed, the precipitation increases the ionospheric electroconductivity and the westward electrojet, which is closed in the equatorial plane and decreases tail currents.

The significance of these processes, which last about 2 hours and form the substorm growth phase, is that they provide the accumulation of the energy excess $\sim 10^{22}$ erg. in the tail and stimulate development of instability there. The latter involve the reconnection around the inner edge of the plasma sheet, which will result in the subsequent release of the accumulated energy and then – in the substorm breakup phase.

Over 10–20 min of the breakup duration, a sharp enhancement of particle precipitation into the auroral ionosphere occurs, in particular of electrons in its morning sector, causing the intensification of the westward auroral electrojet and of field-aligned currents, which close the current in the equatorial tail plane. These currents amount to a threshold value $\sim 10^{-9}$ a cm^{-2}, followed by the occurrence of an anomalous resistivity regime and of field-aligned electric fields, increasing the particle precipitation to a greater extent.

Ionospheric electroconductivity and the westward electrojet are enhanced even more and the latter, being closed in the tail, produces discontinuities in the tail currents. Such tearing implies the reconnection of the tail magnetic field lines and their collapse–recovery to a dipole type. At the same time, the magnetic field

energy stored earlier in the tail is released, and the fluxes of freshly-accelerated particles appear with $W \sim 10$ keV which supports the development of the breakup, which occurs due to instability of the field-aligned currents of the westward electrojet.

The breakup, with the onset in one of the innermost plasma sheet regions around the pre-midnight meridian, extends deep into the tail. This means a poleward expansion and/or drift of the main particle precipitation zone and of auroral electrojets. Electrons transporting the field-aligned currents of the electrojet closure flow out from the plasma sheet at the western end and flow in at the eastern end. Therefore, at the western portion of the plasma sheet, onto which the electrojet is projected, pressure is lowered, resulting in the westward 'partial ring current' of protons and extension of the breakup zone (and the electrojet) in the same direction. Propagation of the breakup deep inside the plasma sheet (up to its outer boundary) and to the west, as well as its gradual decay, is the third and the last substorm period – a recovery phase.

In some details this scheme is close to the UCLA model (McPherron 1974; Coroniti and Kennel 1972a, b 1973), which summarizes the works of many researchers (see the reviews mentioned in the introduction). We would like to note that the growth phase is treated here as a common substorm feature, providing the energy transport of the subsequent breakup from the solar wind into the magnetosphere and its accumulation in the tail, rather than as a specific manifestation of the IMF south component. Just this generalization of the fact of the existence of the growth phase and its well-known signatures were the main reason for a prolonged discussion of the 'growth phase problem', which is still going on.

Note that without such a generalization, some elements of the above scheme would be not included or its substantiation would be weakened, since many of the works whose results are mentioned above were done with no use of information on the IMF.

4.1.3. *Substorms at the North IMF*

Akasofu *et al.* (1973) Akasofu and Kane (1973), and Akasofu (1975a,b) questioned the possibility of generalizing the conclusion on the existence of the substorm growth phase on substorms occurring at the north IMF (or just after it). The important basis for it was the discovery by Akasofu *et al.* (1973) and Akasofu and Kane (1973) of a great number of substorms at the north IMF. The conclusion was made that substorm generation by the solar wind takes place independent of the Z-component of the IMF, which only determines the substorm intensity and aruoral oval dimension: at $B_Z < 0$ the intensity increases and the oval expands, making a substorm available for observations at latitudes $\Phi < 70°$. This conclusion was confirmed and strengthened by Kamide's paper (1974) and is probably undoubted now.

However, Akasofu (1975a,b) has claimed as well that in the analysis of auroral substorms at the north IMF, he had not only not found any growth phase

signatures as mentioned above, but had discovered quite an opposite picture. The conclusions were made that a substorm may follow the northward turning of the IMF, the decrease of a magnetic flux in the tail, thickening of the plasma sheet. These facts evidently, deprive the growth phase signatures described above of a general significance. The growth phase features noted above are such only for the first substorms of the sequence, following the southward IMF turning, and are not the necessary feature of the pre-expansive phase. A real state of readiness for explosion ('the growth phase'), according to Akasofu (1975a), takes place "*always*, except for prolonged periods of a large positive B_Z value". A criterion for readiness of the magnetosphere to generate breakups is the size of the oval; when the area of the latter and the co-latitude of its boundary exceed some values, the magnetic energy stored in the tail appears to be greater than the critical one and the magnetosphere generates breakups (substorms).

The model given by Akasofu (1975a) is not internally contradictory, but it seems to us that the existence of such pre-breakup phenomena as the decrease in the tail magnetic flux and thickening of the plasma sheet are not proved. Due to substorm locality, such evidence could be obtained only in the event of sufficient statistics and also of special methods for data processing.

4.1.4. *Local Features of Substorm Development*

Locality of the development of the westward electrojet – the main element of the substorm current system – was emphasized by Sergeev (1973a,b; 1974a,b) and by Wiens and Rostoker (1975) (see also Troitskaya *et al.*, 1969; Clauer and McPherron 1974a; Vorobjev and Rezhenov 1973; Kisabeth and Rostoker 1973; and others). Wiens and Rostoker have constructed a very convincing picture of the auroral electrojet development.

The electrojet, with a distinctly high latitude and western boundaries, breaks out at the lowest (over the electrojet history) latitudes in the pre-midnight sector ($\Phi = 62$–$68°$). Here it develops during 5–15 min with no appreciable displacements of the indicated boundaries, followed by a new electrojet outburst to the north-west of the previous one. The boundaries of a new electrojet appear to have a stepwise 20–30° departure to the west and few degrees to the north of the preceeding jet. After a certain time lapse ($\approx$10 min), the third electrojet occurs to the north-west of the second one with the same steps in longitude and latitude. This is repeated 4–6 times until the latter electrojet extends to $\Phi \approx 80°$.

In middle and low latitudes a positive bay-like change of the horizontal magnetic field component – a positive bay ΔH with a sharp onset produced by field-aligned currents, entering the jet at the morning side and leaving at the evening side – corresponds to the high-latitude westward electrojet. Wiens and Rostoker (1975) have shown that the onset of a bay at stations with different longitudes experiences a delay that increases to the west in accordance with the westward shift of the electrojet boundary.

The above-mentioned facts are illustrated by few examples but so convincingly that there is no doubt whatsoever as to the reality of these conclusions, which have much in common with Sergeev's results (1973a,b; 1974a,b). However, these authors have reinforced the interpretation of the obtained data. They note that in middle and low latitudes a small negative bay is observed, as a rule, prior to a positive one ΔH. This is an important fact because according to McPherron (1970) and Iijima and Nagata (1972) such a negative bay in ΔH is due to tail currents or field-aligned ones, closing the ring current DRP and, hence, is an indicator of the development of these currents during the growth phase. Having emphasized the latter (a negative bay – an indicator of the growth phase), Wiens and Rostoker pointed out that, on the other hand, due to the above indicated dissimultaneity of the onset of a positive bay ΔH at different longitudes, the following situation takes place. When in one group of stations (eastern) an indicator of the breakup ($+\Delta H$) is seen, at the other stations (western) one can observe at the same time the growth phase ($-\Delta H$). A similar situation was noted by Lezniak and Winckler (1970), using ATS data. In view of this, Wiens and Rostoker made the conclusion that the so-called growth phase usually takes place simultaneously with a breakup and is a consequence of the energy transfer from east to west. So according to these authors, a growth phase does not prepare a breakup but, on the contrary, the growth phase itself as precursor of the expansion phase is put under doubt by the above-mentioned facts.

In his other work Rostoker (1974) finds an example of the growth phase manifestation prior to the breakup phase, but affirms that such examples are not typical.

Thus, Wiens and Rostoker as well as Akasofu (1975a) have come to the conclusion that the existing concept of the substorm growth phase is groundless, and formulate this conclusion in a general form, independent of sign B_Z.

Unlike Akasofu (1975a), who suggests considering the growth phase manifestations as a consequence of IMF $B_Z < 0$ and not as related directly to the substorm, Wiens and Rostoker ignore these known consequences or consider them to be nontypical. In this connection we would like to note that Sergeev (1974a, b), who also discovered local jumplike substorm development, interprets appropriate regularities as arguments in favor of the substorm growth phase concept rather than against it.

The above information shows that the modern concept involves a number of serious controversies and vagueness. Not clear are the real signatures of the pre-expansive substorm phase, i.e. the signature and physical sense of the processes of solar wind energy, mass and momentum transfer to the magnetosphere. It is also not clear whether different types of substorms take place, e.g. at the north and south IMF, or whether they differ only in intensity and in dimensions of the main active region. It is not clear whether the known substorm signatures, e.g. plasma sheet thinning and appearance of the X-type neutral lines, are the cause or consequence of the breakup phase. Finally, the physical sense of

pronounced signatures of the substorm development localities and many other things are quite unclear.

We shall make an attempt to infer additional information about the above problems through the analysis of *magnetic* substorms which unites the main results of substorm studies in the event $B_Z < 0$ (they were briefly noted above) with those of new analyses performed by Mishin *et al.* (1974). This work is concerned with substorms whose initial phase took place during both south and north IMF and, besides, uses a method which enables us to compensate some principal difficulties complicating the description of substorms, owing to their locality and to the insufficient network of stations. Compensation was attained in that the initial data on the magnetic substorm field were derived by specific averaging with the help of the two-dimensional analogue of the epoch superposition method in space Φ, t. In other words, for two groups of normalized substorms, each involving about 50 cases, the expression of current functions $T(\Phi, t)$ were derived through the method described in Section 2. Substorm onsets were uniformly enough distributed in UT so that the original data covered space Φ, t uniformly and densely enough (UT-effects were eliminated by the additional methods). Thus, the incompleteness of the network of stations appeared to be compensated due to the replacement of real (possibly local) disturbances by their average distribution in space Φ, t.

4.2. Magnetic substorms

4.2.1. *Substorm Onset*

Mishin *et al.* (1974) have selected substorms with $\delta H \leqslant 400\gamma$ for analysis, using magnetograms of the morning auroral zone sector. Such an idealized H-magnetogram is illustrated in Figure 21 where the separation of substorms into subphases is also shown. The selected 93 substorms of season V-VIII, 1968 were divided into two groups (47 and 46) according to sign B_Y of the IMF. It turned out that in the pre-breakup phase $\tau = 1.4$) these two groups differed also in sign IMF B_Z (see Figure 21b,c). For each subphase the systems of equivalent currents $\Delta T(\Phi, t) = T(\Phi, t) - T_q(\Phi, t)$ were computed, where values T_q correspond to the level of quiet days. Values of the j-current density module, used as a suitable measure of local substorm intensity, were derived as well.

An average substorm of the away IMF sector ($B_Y < 0$) is represented in Figure 22 by curves $j(\tau)$ at the uniform grid of points in space Φ, t. One can see that the sharp growth of j in the pre-midnight sector of the auroral zone corresponds to the onset of the breakup phase, i.e. to instant $\tau = 4$ on figure 21. (See arrows in sector 23–04$^h LT$, $\Phi = 66$–$68°$.) Moving step by step from the auroral zone upward in latitude, one can easily determine similar onset moments outside the auroral zone as well, though they are less pronounced here. (In sector 8–10$^h LT$ at $\Phi = 76$–$80°$ the moment $\tau = 1$ is taken as a substorm onset since at this very moment $j > 200$ a km$^{-1} \geqslant 0.5$ j max.) In such a way, the onsets (connected in

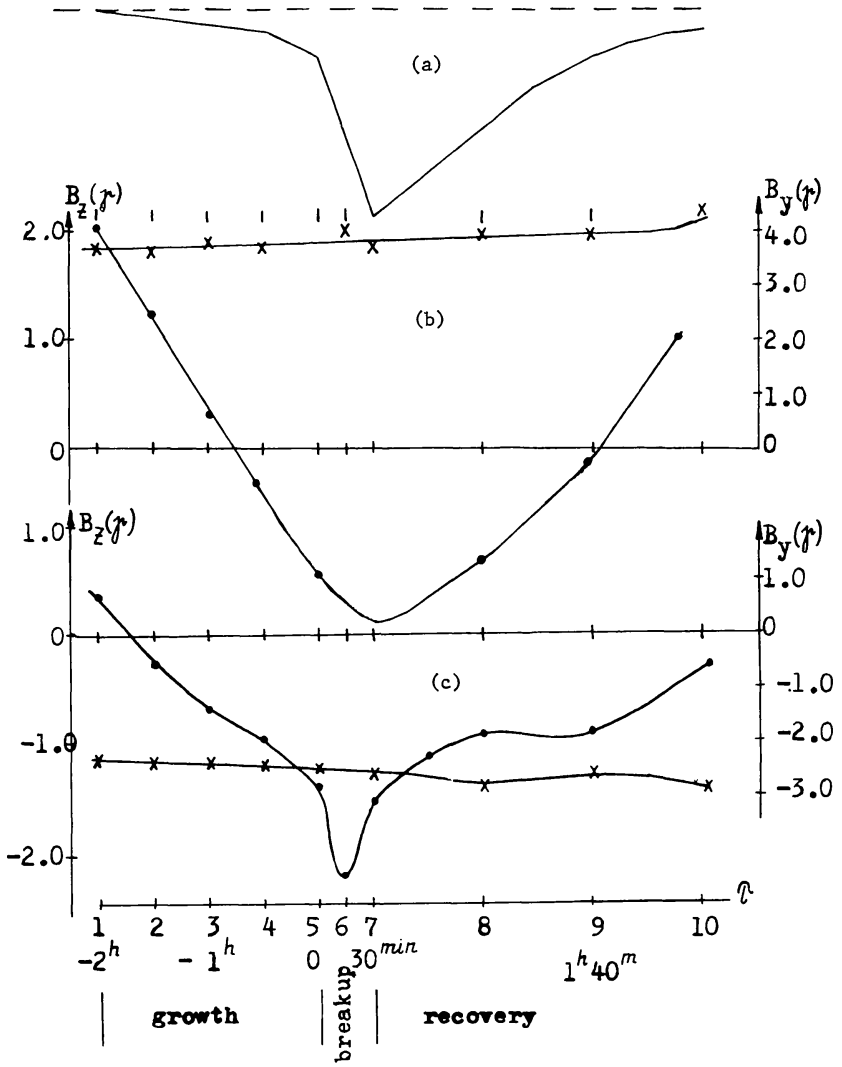

Fig. 21. (a) The idealized H-magnetogram of a substorm in the early morning sector of the auroral zone ($\Phi = 64$–$68°$); (b) mean values of IMF B_z (dots) and B_y (crosses) for substorms of the away sector; (c) the same for the toward sector. Abscissae – substorm time τ moments $\tau = 1.10$ are indicated.

Figure 22 by dotted lines) are determined. They reveal a distinct enough tendency: with increasing latitude a visible substorm onset shifts, as a rule, from $\tau = 4.5$ in the auroral zone to $\tau = 1.2$ at $\Phi = 76$–$80°$. This is illustrated also in Figure 23 by the patterns of distribution of 'onsets' in space Φ, t where the zone of the first, i.e. real, substorm onset is shaded. If, for the sake of simplicity, we temporarily ignore some features, then two independent samples of substorms, presented in Figure 23a,b, would reveal similar and distinct enough regularities. The 'real' substorm onset is seen to occur 1.5–2 hours prior to the breakup moment in the auroral zone. The region of real substorm onset is located in the first approximation at $\Phi = 75$–$80°$, i.e. in the same area where the polar electrojet is flowing at quiet periods (Figure 11). It is important that the shape of the 'substorm onset zone' appears to be mostly independent of the IMF sign B_Z,

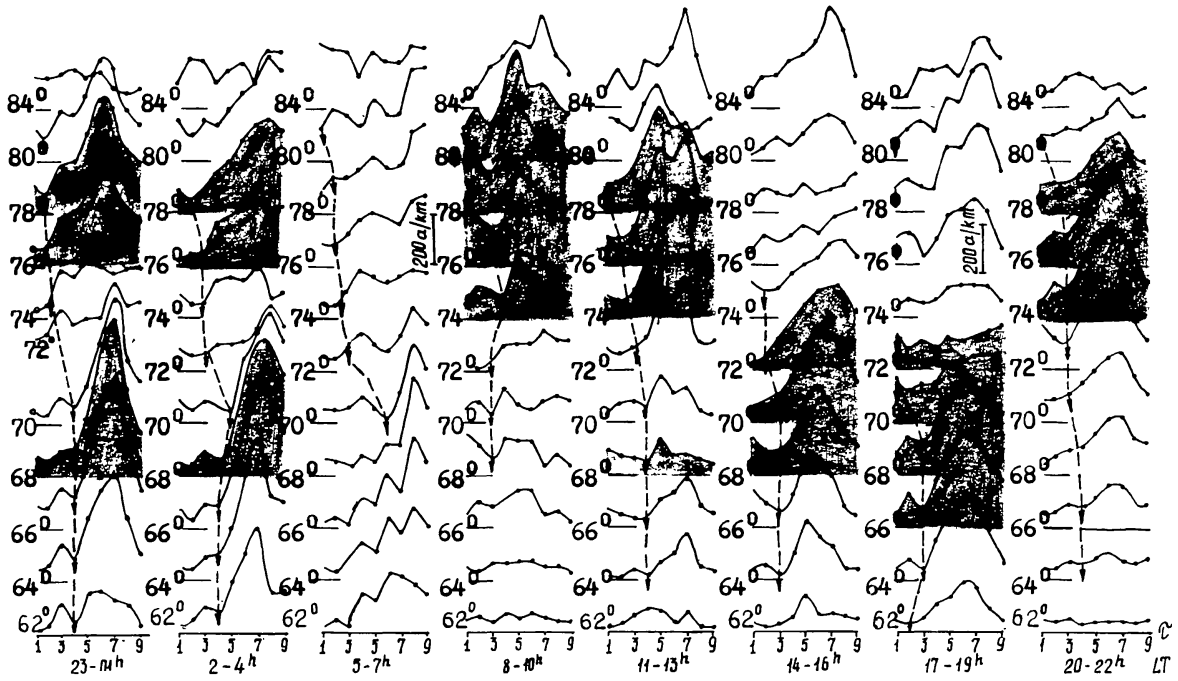

Fig. 22 Abscissae – substorm time τ, ordinates – density of the equivalent substorm current in the away IMF sector. LT-intervals are shown at the bottom. Regions of polar and auroral electrojets are shaded. Moments of the substorm onset (arrows) are connected by dotted lines. You can see that the onset moment tends to shift from $\tau = 1.2$ at $\Phi = 74$–$80°$ to $\tau = 3$–5 at $\Phi < 70°$.

though at the north IMF the mean latitude of this zone is several degrees higher than at the south one.

As noted in Section 3.2, the origin of the quiet polar electrojet may be understood as a result of the transfer of solar wind electric field $-\mathbf{V} \times \mathbf{B}$ into the ionosphere along the tail geomagnetic field lines. The presence of the nighttime maximum of the polar electrojet density (Figure 11) requires the magnetospheric cleft, responsible for the maximum in the projected electric field, to take place at the night side too, that is, to be closed at the quiet period. So, Figure 11 shows a magnetospheric cleft, observed both at the day and night sides, as distinct from the dayside cusp, limited in longitude. One can easily see that in the first approximation, Figure 23 also corresponds to the model magnetospheric cleft, observed at about $\Phi \approx 78°$ on the day and night sides.

Though Figure 23 examined separately enables us to speak about the region of the first solar wind contact with the geomagnetosphere rather than about the cleft, the term 'cleft' seems to be quite suitable. Indeed, the first contact corresponds to the magnetopause and the last (in the open magnetosphere model) is the outer 'cleft' boundary. One more reasonable fact is that 'the zone of onsets' in Figure 23 coincides with the 'inner' one of magnetic activity maximum and with the maximum of the 'soft' zone of particle precipitation into the ionosphere (Vershinina 1966; Mishin 1962; Mishin *et al.*, 1970, 1971; Hoffman 1970; Hoffman and Burch 1973). According to the available interpretation of these zones, they coincide with the magnetospheric cleft projection (Mishin and Saifudinova 1968;

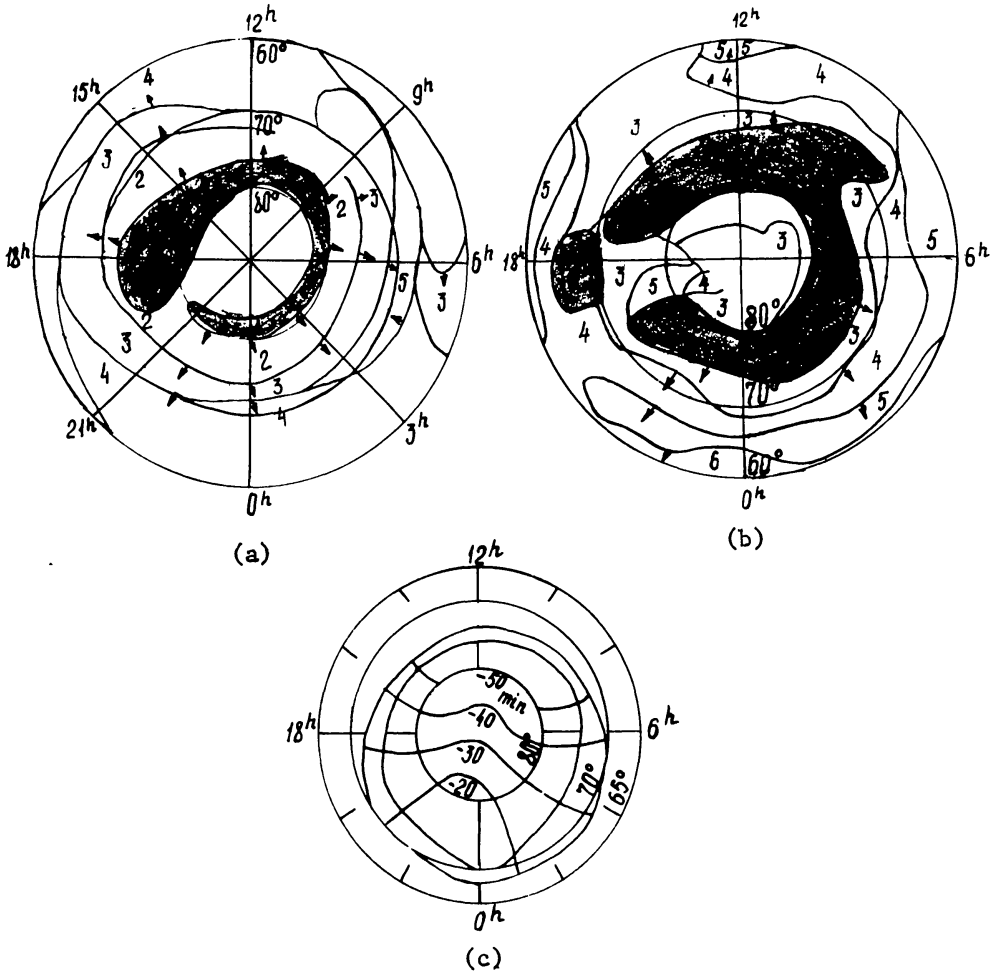

Fig. 23 Distribution of substorm onset moments in coordinates Φ,t for the away (a) and toward (b) IMF sectors on data by Mishin *et al.* (1974). Ciphers, connected by isolines, are the numbers of moments τ (Figure 21). A zone of the primary onset ($\tau = 1.2$) is shaded. Arrows indicate the direction of the expansion of the zone of onsets. *Bottom:* (b) – development of a substorm on data by Iijima (1974). The auroral oval and isochrones of the disturbance commencement are shown. Time is reckoned from breakup.

Mishin *et al.*, 1970; Russell *et al.*, 1974). In this case the cleft should be closed because the 'inner zone' is observed at all LT-meridians. A similar conclusion, though based on some other ideas on intrusion zones, was drawn by Feldstein and Starkov (1970). They concluded that the boundary between closed and open field lines corresponds to a polar boundary of the auroral oval ($\Phi = 74$–$75°$ (see also Coroniti and Kennel 1971).

Note that a magnetosphere model in Figure 13 does not involve a magnetospheric cleft as a boundary between closed and 'open' field lines since this term is not used in the model. However, latitudes near $\Phi = 78°$ in this model are distinguished as being topologically specific at all LT-meridians, nightside ones included. So, a conclusion on the existence of a magnetospheric cleft whose projection corresponds to $\Phi = 75$–$80°$ within a wide LT-range from midnoon to midnight is not contradictory to the relevant magnetosphere model, though it does not follow from it.

Thus, a substorm occurs 1.5–2 hours prior to a breakup in the area, the main part of which is a projection of a magnetospheric cleft at $\Phi = 75$–$80°$ in the pre-midnoon, morning and pre-midnight hours. In the dusk sector (14–$21^h LT$) a zone of onsets is close to a spiral – a portion of the auroral oval, projected onto the region, close to the inner edge of the plasma sheet and to the region of partial ring current occurrence. This feature is associated with the above conclusions by Iijima and Nagata (1972); however, the nature of the dusk portion of the zone of onsets – is not clear.

4.2.1.1. *Polar electrojet.* A substorm onset in the polar cap, occurring prior to the auroral breakup, was first noted by Oguti (1969). He observed that 30–40 min before a breakup a current filament appears at the dayside of the oval which produces 'magnetic peaks' at the Earth's surface – baylike disturbances with $\delta H \sim 50\gamma$ and with a quasi-period ~20 min. This current filament shifts toward the auroral zone and reaches its nightside portion at the instant $T = 0$. In Figure 23c a similar result, based on Iijima's data (1974), is shown. These data confirm that the substorm growth around the magnetopause takes place much earlier than near the inner plasma sheet edge, but that it corresponds to the dayside cusp model rather than to the real (closed) magnetospheric cleft. The disturbance in Figure 23c propagates across the tail lobes whereas in Figures 23a,b – from the outer plasma sheet boundary (around the magnetopause) to the inner one. Such propagation takes place both in the daytime and nighttime hours, but most distinctly in the latter case.

Figure 24 illustrates a magnetospheric cleft signature at different substorm phases, including 1–2 hours prior to the breakup, by one more example, characterizing the dependence $j(\Phi)$ in the away sector of the IMF. One can see that the cleft zone ($\Phi = 75$–$80°$) at all LT-hours excluding the evening ones and at all substorm phases is distinguished (like the auroral zone after the breakup) with increased values of current density j. Maximum values dj/dT, noted in the previous section for instants $\tau = 1.2$, yield here at $\tau = 3.4$ and then the maximum quantities of value j itself, which corresponds to the polar electrojet occurrence. Note that the polar electrojet in Figure 24 is distinguished after the subtraction of field S_q^p, i.e. *this electrojet is a new element of the substorm field.* It was pointed out earlier by Mishina (1970), Mishin *et al.* (1970) as part of current systems *SD*. Still earlier, as noted, a zone $\Phi = 75$–$80°$ was selected as the zone of maximum magnetic activity, i.e. of fluctuation portion of function j (Φ, t). Balloon measurements of the electric field above Thule (Mozer *et al.*, 1974) also support that with increasing magnetic disturbances the contribution made by the Y-component of the IMF to the electric field is sharply enhanced. This enhancement at the daytime is ~50 mv; a compatible effect was noted in the paper by Mozer *et al.* (Figures 10, 12) at the nighttime, too.

Their data enable us to suggest that a portion of the polar substorm electrojet has the same origin as on quiet days, i.e. it is a Hall current induced by the

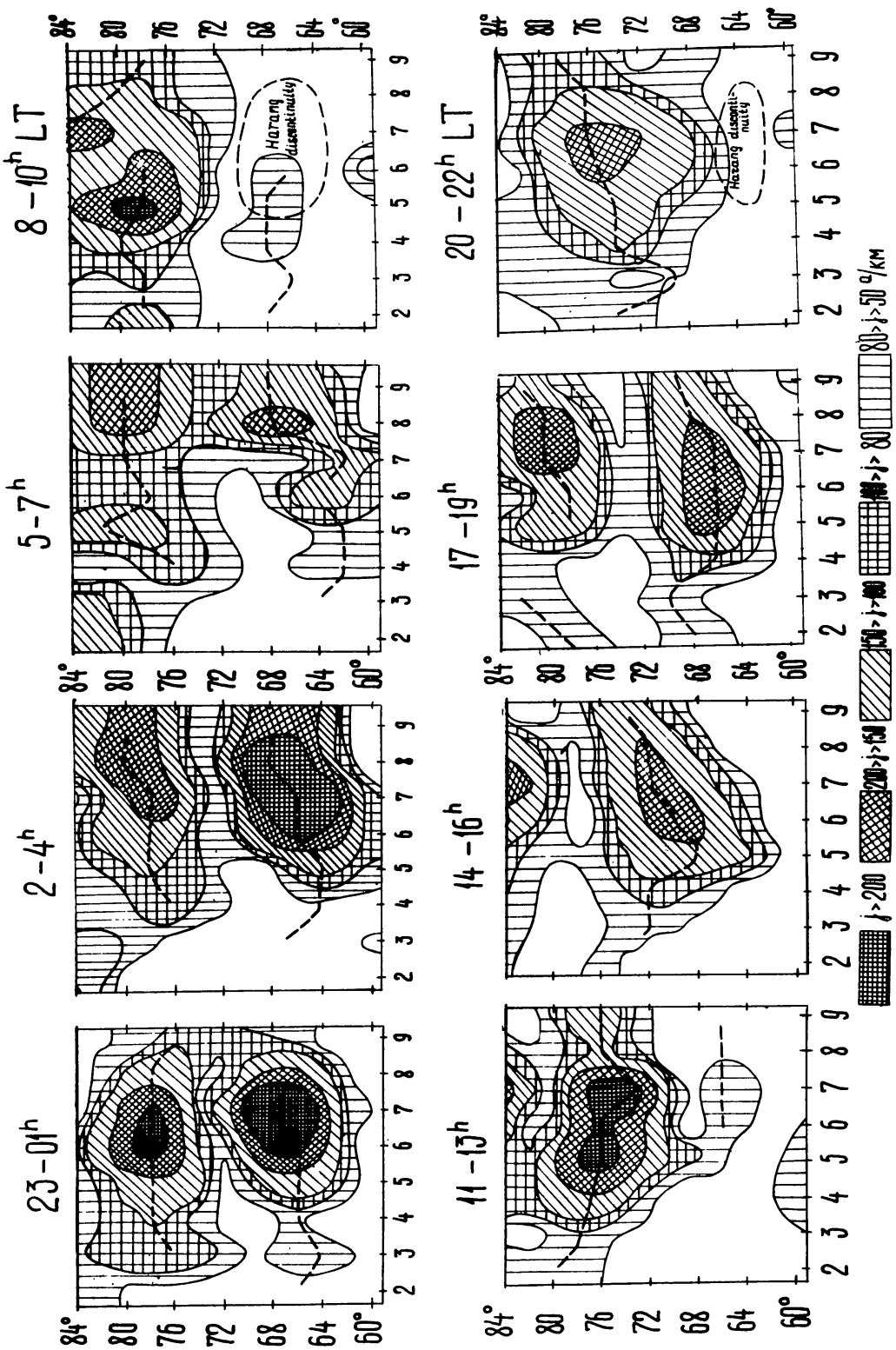

Fig. 24. The module of substorm current density in coordinates Φ, τ for the away IMF sector. LT-intervals are indicated too. One can see that maximum values j display a polar electrojet near $\Phi = 75$–$80°$ and two auroral electrojets in the dawn sector near $\Phi \approx 67°$ and in the dusk one – along a spiral, connecting 75 and 65°.

meridional component of field $-\mathbf{V}\times\mathbf{B}_Y$. This is supported as well by the following data.

(a) As shown by additional analysis of data in Figure 25, the difference of currents at $\Phi = 75$–$80°$, obtained at $B_Y > 0$ and $B_Y < 0$, is an eastward current predominant around midnoon and in the morning. Just such a direction should be peculiar to this difference of currents if the polar electrojet is a Hall current generated by the field $-\mathbf{V}\times\mathbf{B}_Y$.

(b) A comparison of two current systems in Figure 25 shows that the ratio of intensities of the dawn and dusk vortices changes with sign B_Y. At $B_Y > 0$ the dusk vortex is predominant and at $B_Y < 0$ the dawn one, like that it takes place in S_q^P due to the presence of the Hall polar electrojet, produced by the meridional portion of field $-\mathbf{V}\times\mathbf{B}_Y$.

However, the nature of the polar electrojet during a substorm is obviously more complex than on quiet days.

In the pre-midnight sector the polar electrojet in Figure 25 is directed eastward, irrespective of sign B_Y. At this period the contribution of closing currents of the westward auroral electrojet is evidently predominant in it, which is more clearly seen on data of the substorm breakup phase (Section 4.2.2). It follows that if on quiet days the polar electrojet occurs within $\Phi = 75$–$80°$ as a result of focusing and enhancement of the meridional portion of electric field $-\mathbf{V}\times\mathbf{B}_Y$ there, its second main cause during substorms is the appearance of the electroconductivity maximum, i.e. coincidence of the magnetospheric cleft zone with the 'inner' (soft) one of the corpuscular intrusion intensity maximum. The second cause prevails and manifests itself very clearly during the night hours, emphasizing still more the difference between the magnetospheric cleft and the 'dayside cusp'.

The development of the polar electrojet during a substorm is illustrated in Figure 26. In the early morning these variations are mostly caused by ionospheric electroconductivity fluctuations, and during the day by changes in magnetospheric cleft parameters. In particular, Figure 24 shows for the pre-midnoon hours that from $\tau = 1$–2 to $\tau = 4$ the center of the cleft, identified by the maximum of j (dotted line), shifts from $\Phi = 80°$ to $\Phi = 74°$, that occurs, with reference to Figure 21, parallel to the IMF south component growth in accordance with Burch's results (1973).

4.2.1.2. *The enhancement of magnetospheric convection and currents DP-2.* Iijima and Nagata (1968), Iijima *et al.* (1968), and Iijima (1968) have demonstrated that nearly an hour prior to the breakup a polar two-vortex current system is enhanced like the S_q^P one. According to modern terminology, it means the appearance of the high-latitude portion of currents *DP*-2, introduced by Nishida *et al.* (1966). Similar results were obtained later by Oguti (1969), Ivliev *et al.* (1970), Mishin and Grafe (1971), Kokubun (1971), Iijima and Nagata (1972). However, all these results were obtained either with no use of data on IMF B_z or for cases $B_Z < 0$.

Using data by Mishin *et al.* (1974) the analogous results are illustrated by

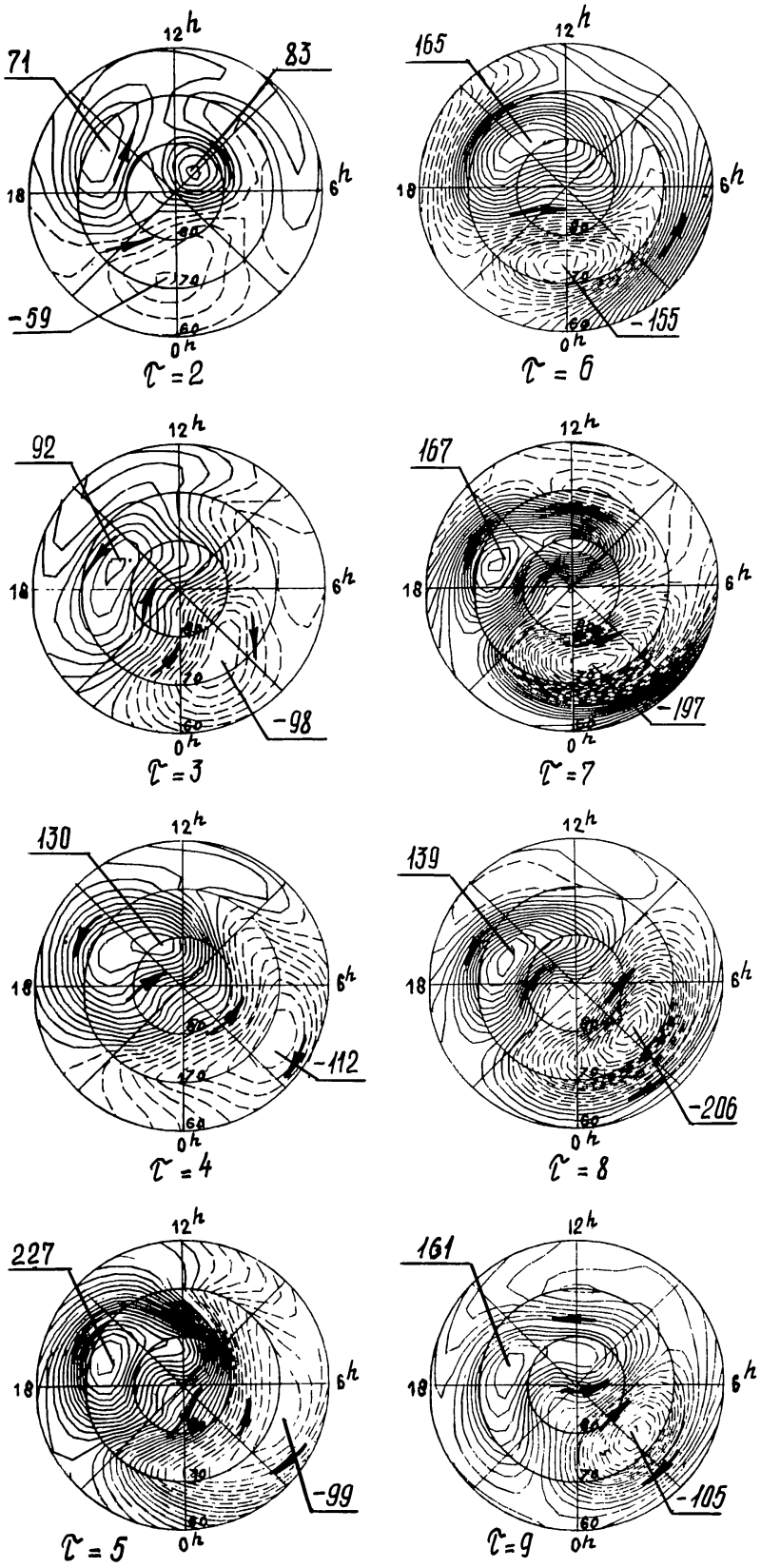

(a)

Fig. 25. Systems of equivalent currents for substorms in the away (a) and toward (b) IMF sectors. Coordinates – geomagnetic latitude and time, focal values – in kiloamperes.

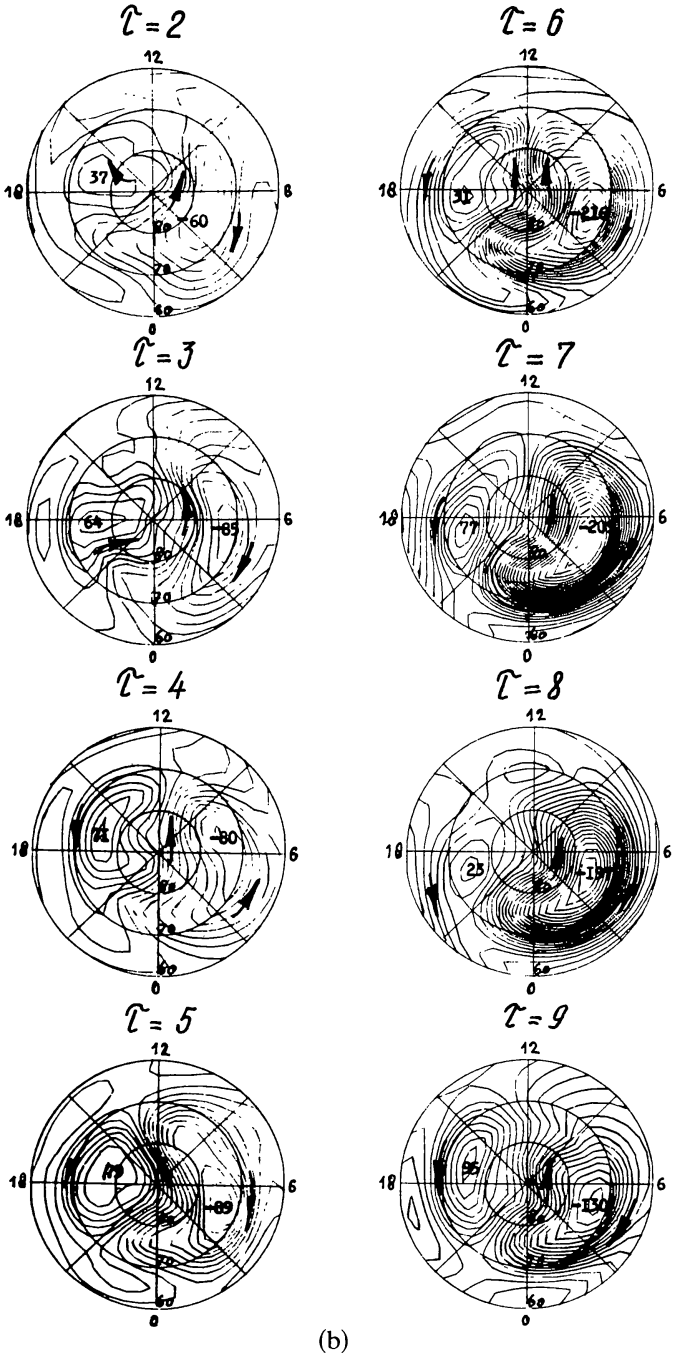

(b)

Fig. 25 (*cont'd*).

Figures 24–26 where the systems of equivalent currents of individual substorm phases are schematically represented, as well as the distribution of their density module for cases $B_Z < 0$ and $B_Z \geqslant 0$. If one interprets the equivalent current in Figures 25 in the first approximation as a Hall current, one may emphasize the following.

At the very onset of the growth phase ($\tau \leq 2$) a substorm current system is rather complex but, nevertheless, it admits the interpretation within the framework of a common scheme. Indeed, at the instant $\tau = 2$ in zone $\Phi = 75$–$80°$ (a magnetospheric cleft) Figure 25a shows currents which form on the dayside two distinct electrojets, corresponding to convection, directed away from the Sun. A

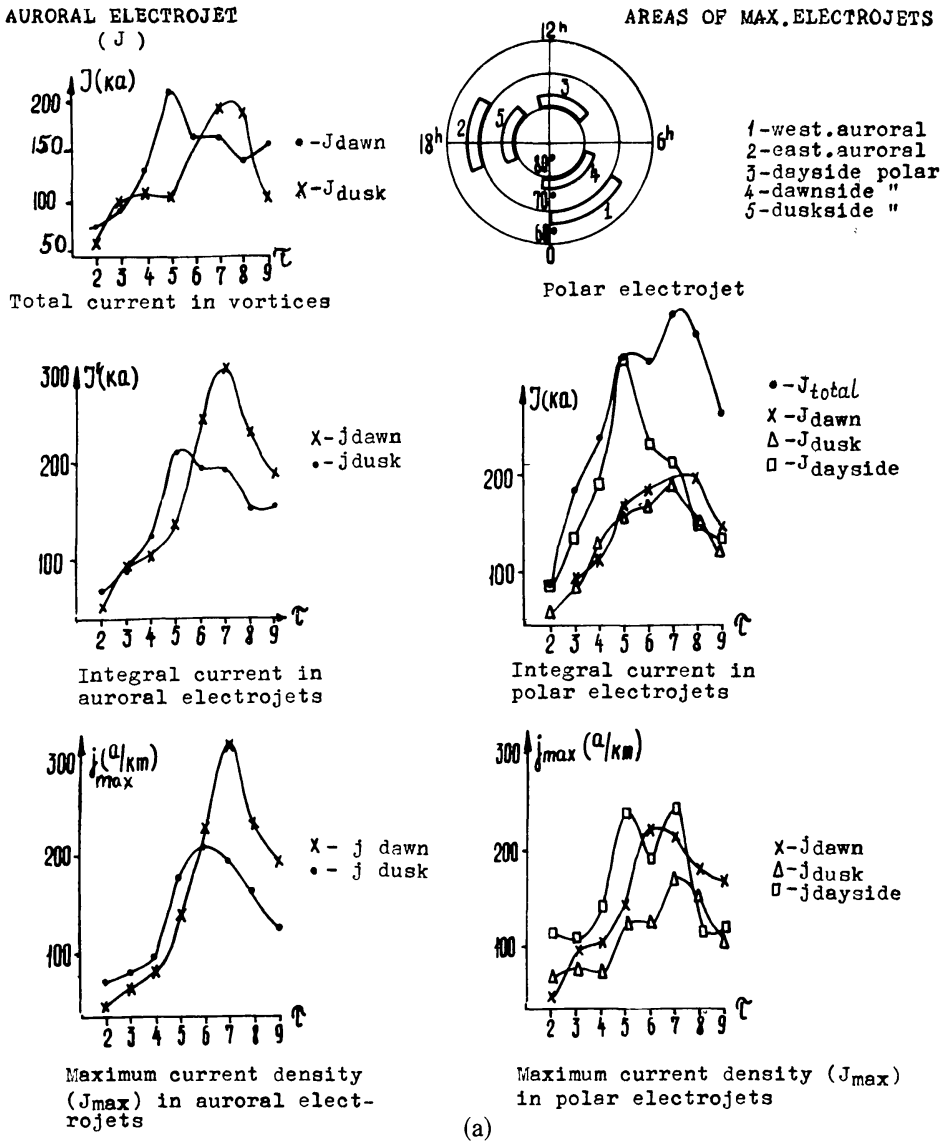

Fig. 26. Development of main electrojets and current vortices in substorms of the toward (a) and away (b) IMF sectors.

In the upper right corner – main portions of electrojets. Abscissae – substorm time τ (Figure 21). The integral current in electrojets is obtained by summation of values $j \geq 0.5\ j_{max}$. Value j_{total} in (a) of this Figure is a total current across the northern polar cap.

specific feature of this initial growth phase moment is that the anti-solar convection covers not the entire polar cap, including tail lobes, but is concentrated in the narrow magnetospheric boundary layer, i.e. is developed only partially. A return convection at $\Phi = 65$–$70°$ is concentrated also on the dayside (and in the around polar region), i.e. as compared with the common *DP*-2 system, and is also developed only partially; *on the nightside*, within the latitude region, corresponding to a plasma sheet, *a return convection is absent.* This fact supports the suggestion made by Coroniti and Kennel (1972a): the predominance of anti-solar convection over the return one provides the accumulation of magnetic energy and plasma in the magnetotail.

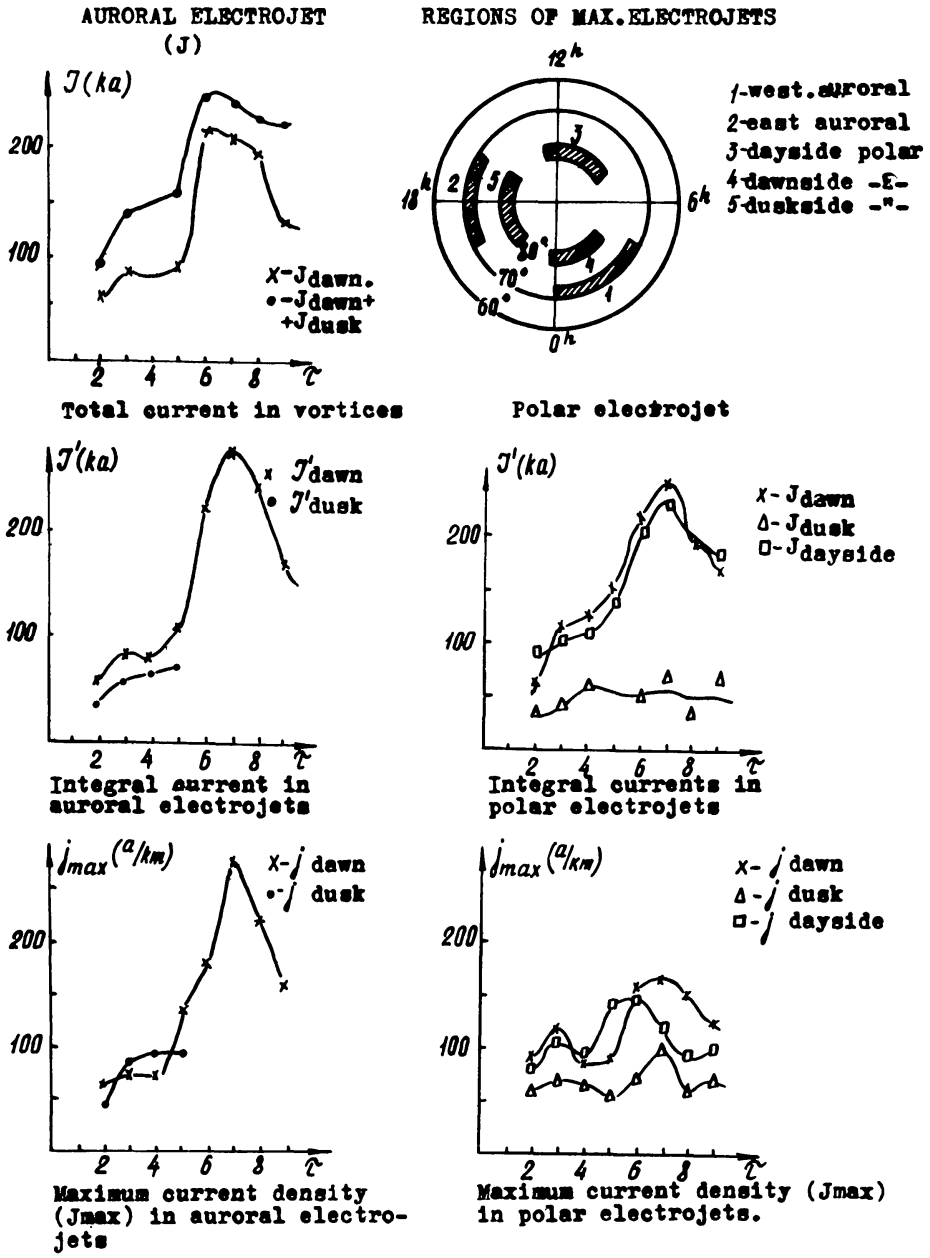

(b)

Fig. 26. (*cont'd*).

Further on, at the instants $\tau = 3$–5 not only does the increase of intensity of two convection vortices occur, but their shape becomes close to the usual form of the *DP*-2 system too. A temporary history of the convection development is illustrated by curve T_{dusk} (τ) in Figure 26a (in the dawn vortex the contribution of field-aligned currents of the westward auroral electrojets is great – Langel (1974)). The maximum of convection development is seen to occur at the end of the growth phase, ~30 min before a maximum development of substorm currents is achieved. Hence, the latter are enhanced during the breakup phase due to the electroconductivity (via particle precipitation) but not due to subsequent growth of the electric field.

Particle precipitation in the auroral zone ($\Phi = 65$–$78°$) is slightly enhanced also in the pre-breakup phase (Pytte and Trefall 1971; Hones *et al.* 1971; Axford 1969; Hargreaves *et al.* 1975). As noted by Iijima and Nagata (1968), McPherron (1970), Iijima (1972a), Iijima and Nagata (1972) and others, this is consistent with the growth of auroral electrojets at $\Phi = 65$–$70°$ – eastward in the dusk and westward in the dawn sectors of the above-mentioned two-vortex system of Hall currents. These electrojets are also seen on data of Figures 24, 25, and 28. Figure 25a shows e.g. that beginning from the instant $\tau = 2$ return convection produces the eastward electrojet at about $\Phi = 70°$ between 16 and $19^h LT$, and from $\tau = 3$ a westward electrojet in the dawn sector of the same latitude zone, which is projected onto the inner edge of the plasma sheet.

Time development of auroral electrojets is illustrated also in Figure 28, taken from the work by Iijima and Nagata (1972). One can see that at the pre-breakup period the eastward electrojet (and indices AU) are developed faster than the westward one (and indices AL). According to Iijima and Nagata (1972), this implies the predominant development of the partial ring current DRP during the growth phase (see Troshichev *et al.*, 1974).

4.2.1.3. '*Dawn–dusk*' *inequalities.* Figure 27 shows that near the polar cap boundaries j-values of equivalent current density in the away IMF sector are greater in the morning than in the evening; in the toward sector this difference changes its sign or disappears. Table I (for the pre-breakup phase and $\tau = 7$) shows that the above 'dawn-dusk' inequalities take place in the electric field $E = j/\Sigma_H$ too, where Σ_H is the integral Hall conductivity (Osipova and Vanjan, 1975). This is consistent with Heppner's results (1972) and points to the contribution of IMF B_Y (see Section 3.2.).

This Table also permits us to draw a conclusion about the effect of the X-component of the IMF: LT-meridians with the greatest electric field gradients rotate with the transition from $B_X > 0$ to $B_X < 0$ in such a manner as was predicted by Stern's model (1973) (see Figure 6).

4.2.2. *Breakup and Recovery Phases. A Fine Structure of Substorms*

In Figure 29 one can see that a region of the westward electrojet with maximum density was localized in the dawn sector at the very onset of the growth phase and gradually moved to the west, together with its reflection in the nightside part of the polar electrojet up to $\tau = 4$. At the instant $\tau = 4$ this westward drift discontinues at $LT = 23^h$ with a subsequent change of its sign. Figure 22 shows that at the same time here ($LT = 23^h$) and in the early morning sector there is the sharpest enhancement of the westward electrojet. Thus, the onset of a breakup may be localized as an event at about $\tau = 4$, most prominent in zone $\Phi = 66$–$70°$, $LT = 22$–$4^h LT$. The maximum density of the westward electrojet at this moment is near $LT = 22$–$23^h LT$, which corresponds to a zone of neutral line formation after Nishida and Hones (1974).

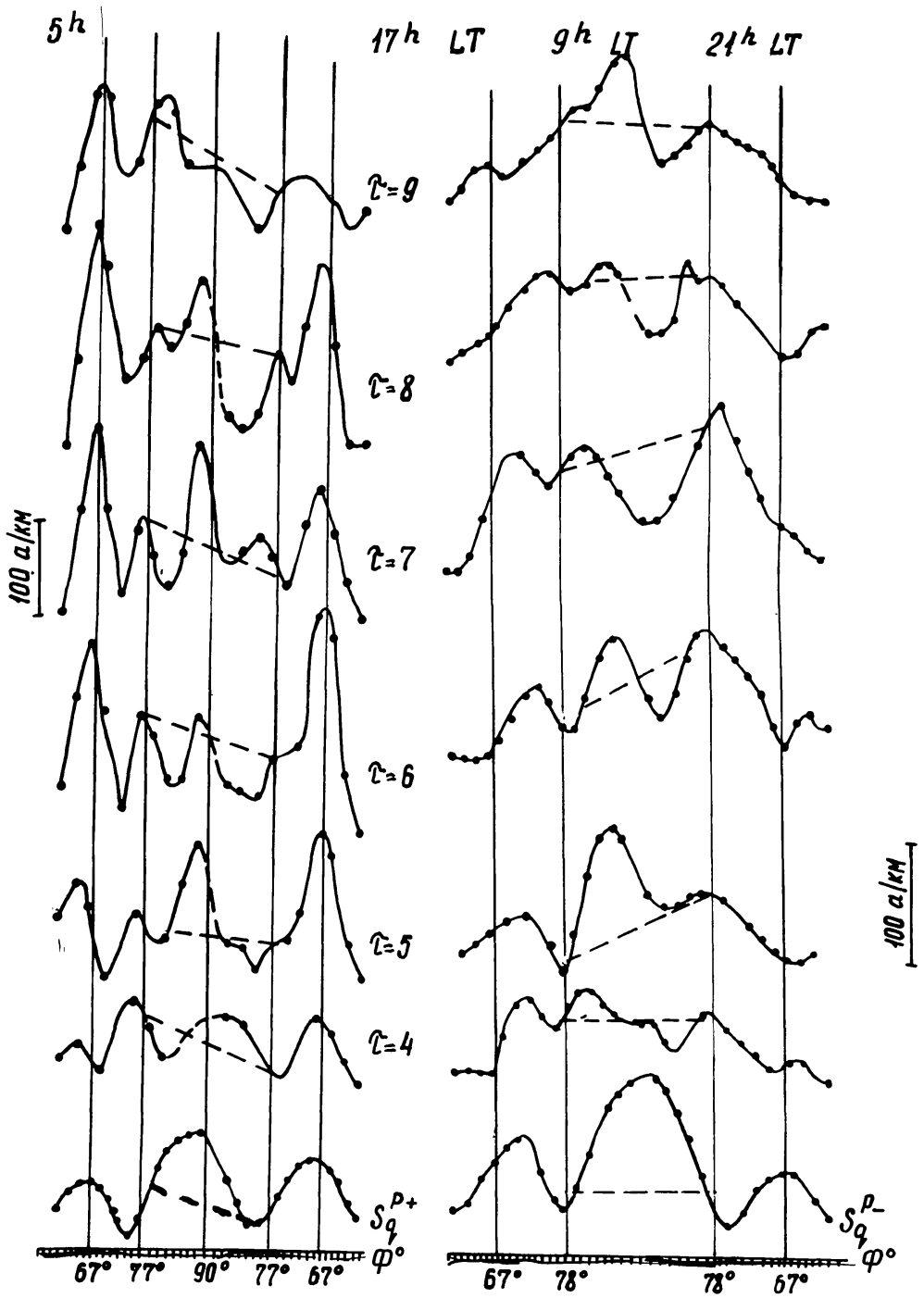

Fig. 27. Values of density module of equivalent substorm currents for the away (left) and toward (right) IMF sectors, plotted against geomagnetic latitude Φ for two dawn–dusk LT-meridians, indicated at the top. Values j at the polar cap boundaries ($\Phi = 78$–$82°$) are connected by dashed lines.

One can see that in the away IMF sector the morning values tend to exceed the evening ones. In the toward sector this difference disappears or alters its sign, which corresponds to the predominance of the dusk current vortex in the former case and of the dawn one in the latter case.

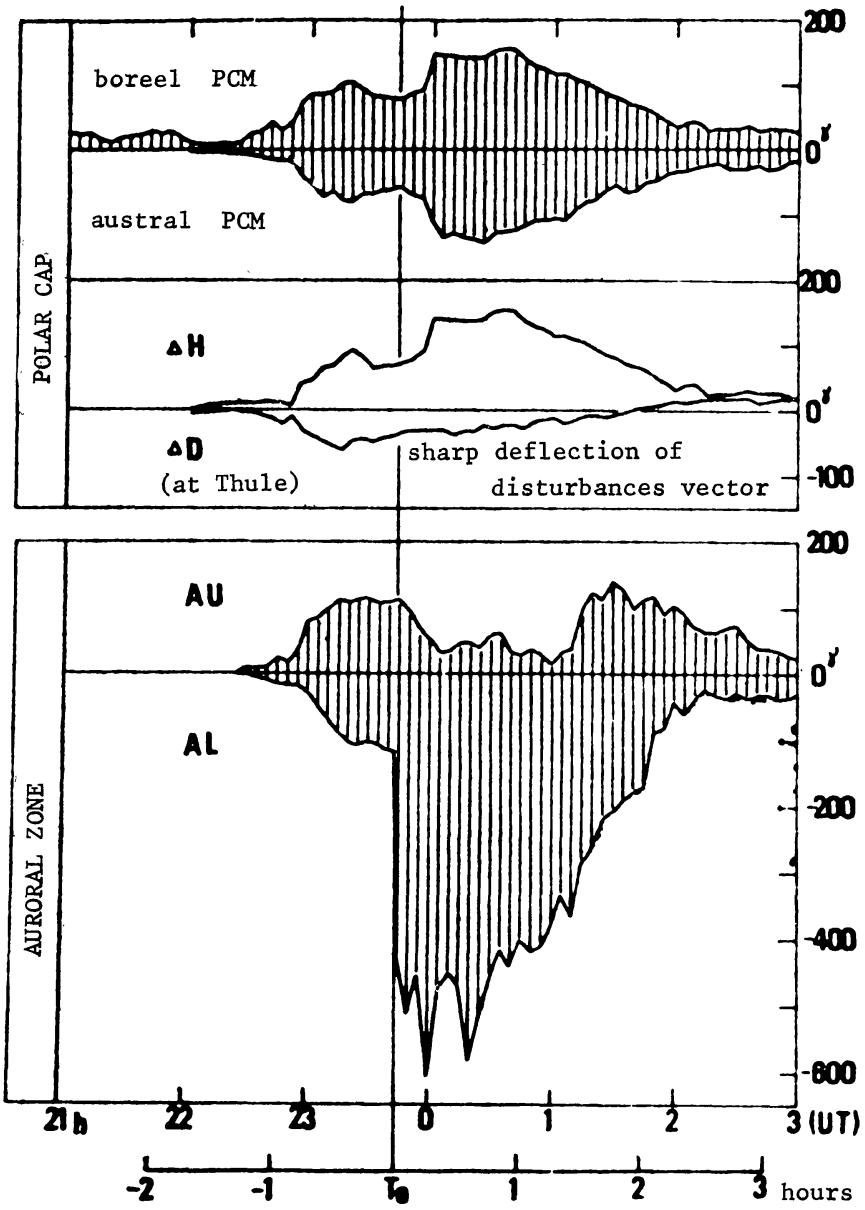

Fig. 28. Magnetic activity characteristics for a substorm of 12–13 September, 1958 (every 5 min). *Top:* PCM indices, i.e. mean disturbance vectors ΔH in the northern and southern near-pole regions ($\Phi \geq 85°$), and H, D–magnetograms from Thule. *Bottom: AU* and *AL* indices. (after Iijima (1972b)).

The subsequent development of an expansion phase is mainly the enhancement of the westward electrojet and the motions of its boundaries, as well as of the region of maximum current density. During 10–30 min of the breakup phase the intensity of the westward electrojet is enhanced several times. In Figure 26a it amounts to 300 kA, indicating a relatively weak intensity of the mean substorm, examined by Mishin *et al.* (1974). The closing of the westward electrojet occurs, mostly, through the eastward current in the nightside portion of zone $\Phi = 75–80°$. This closing current forms the nightside portion of the polar electrojet which drifts with τ, as shown in Figure 29. Hence, the morning vortex of the equivalent

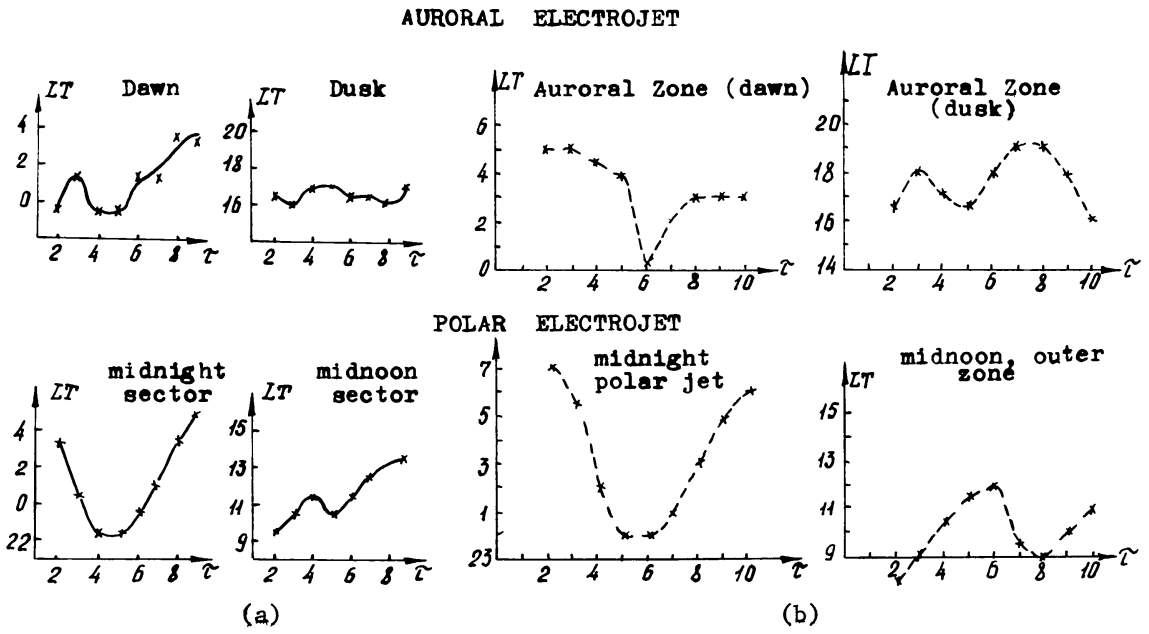

Fig. 29. Abscissae – substorm phases, ordinates – local time of the maximum of electrojets in substorms for the away (a) and toward (b) IMF sectors.

substorm currents is not a current along the auroral oval. The fact that equivalent currents of the closing of the westward electrojet are *concentrated* in the narrow zone $\Phi = 75$–$80°$ and are *directed* as the expected closing currents but not as currents equivalent to field-aligned ones, permits us to conclude with confidence that a considerable part of the westward electrojet (a Cowling current) is really closed in the nightside polar ionosphere.

Together with the westward auroral electrojet during the breakup, the eastward and polar electrojets are also enhanced, though weaker. The regions of maximum density of the westward and polar electrojets are drifting eastward, as shown in Figure 29, with a velocity close to that of the gradient drift of 10–keV electrons.

In Figure 24 one can see that in the dawn sector the northern boundary of the westward electrojet experiences a poleward shift. However, the averaging of the original data and the method through which these data were obtained could make the results somewhat rough and misleading. Therefore we shall refer in addition to the analysis of individual cases performed by Wiens and Rostoker (1975). They have shown that a jumplike displacement of the northern boundary of the westward electrojet is sometimes observed up to $\Phi = 80°$ which corresponds to the outer plasma sheet boundary. As already noted, the data of midlatitude stations made it possible for Wiens and Rostoker to also conclude that the western boundary of the electrojet shifts westward in a steplike fashion like the northern one with a velocity of 20–30° per one step. Rostoker and Kisabeth (1973) have noted that the southern boundary and the center of electrojet remain stable.

When the disturbance wave (observed as a northern boundary of the westward electrojet or as a maximum of aurora luminosity) reaches the outer plasma sheet

boundary, then the post-breakup can occur in this location, after which a magnetic bay and/or aurorae are again moving, relaxing, toward the inner plasma sheet boundary (Hirasawa and Nagata 1972; Wiens and Rostoker 1975, Figure 2). This phenomenon is evidently triggered by the ejection of plasma from the nightside polar cusp – a portion of the closed magnetospheric cleft. Thus, the post-breakup at $\Phi = 76$–$80°$ supports the cleft model described above (see also Winningham *et al.*, 1975). Such an interpretation also makes it possible to confirm though indirectly, the supposition by Nishida and Hones (1974) that the development of the breakup, propagating to the distant plasma sheet after the neutral line formation in its near portion, occurs after the neutral line disappearance, i.e. due to kinetic plasma energy accumulated at drift shells of the plasma sheet (but not resulting from reconnection and annihilation of a magnetic field).

In this case the term 'breakup, propagating to the distant tail' is not completely correct, since the breakup is associated with neutral line formation but the motion toward the outer plasma sheet boundary – with essentially other process of precipitation of particles, being trapped earlier. Then the onset of the recovery phase is the beginning of the poleward drift of the westward electrojet or the moment of the first jump, after Wiens and Rostoker (1975).

Along with the above-mentioned steplike expansion of the westward electrojet there are many other signatures of local substorm development. So, for instance, Nadubovich (1967) has discovered a coastal effect of aurorae – a statistically significant tendency of auroral arcs to occur more frequently above the coastal line of the Laptev sea than in the sea or far from the shore. A similar coastal effect in distribution of the external equivalent substorm currents is illustrated in Figure 30. The estimation of correlation between the coastal and current lines confirms a high statistical significance of the effect. The other signature of substorm development locality is the 'effect of patchiness' of aurorae (Samsonov 1971). It means that isolines ρ – probability of aurora occurrence above Yakutia – form patches with sharply differing ρ-values and with characteristic dimensions of nonuniformity ~500–1000 km, displaying a significant positive correlation with distribution of geomagnetic field intensity at E-layer height. Since magnetic field inhomogeneities decrease as R^{-n}, where (in the given case) $n > 20$, they fade at small distances from the Earth's surface. It implies that a breakup trigger, distinguishing its manifestation in small spatial regions, is localized not in the plasma sheet (far away from the Earth) but in the ionosphere, at $h \sim 1000$ km. Such a process may be, as is known, the instability of field-aligned currents caused by the generation of ion àcoustic waves and by the occurrence of anomalous resistivity (Oguti 1971; Atkinson 1970; Coroniti and Kennel 1972b) and may not be, regarded separately, the ion tearing mechanism (Schindler 1974; Galeev and Zeleny 1975).

On the other hand, Figure 31 shows a small auroral substorm of the 'contracted oval', recorded at Golomyany station ($\Phi = 74°$) on January 31, 1973. It is of interest because it is not accompanied by a magnetic disturbance and, hence, may

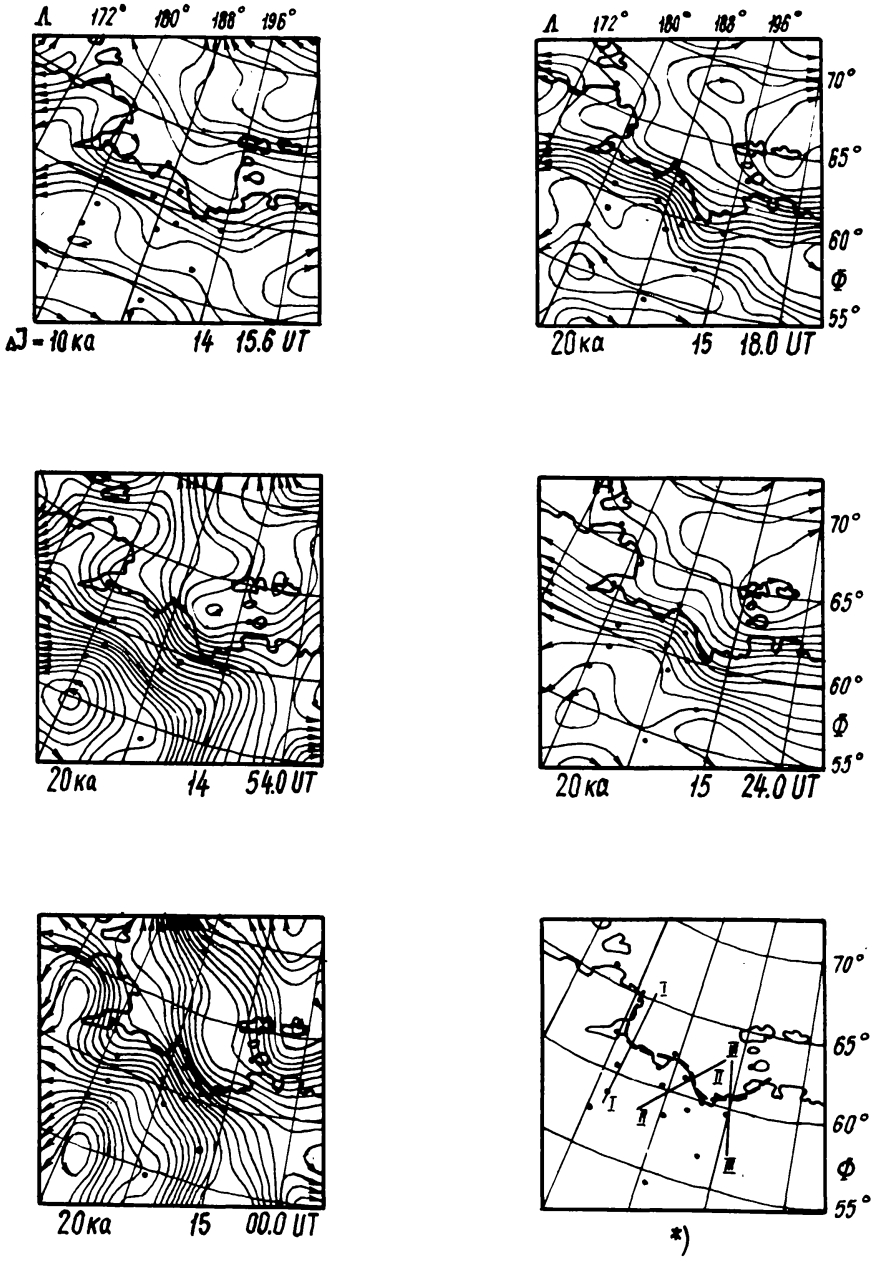

Fig. 30. Equivalent currents of a substorm at 14–16^{h}UT on January 26, 1969 on data of a dense network of stations (shown by dots). Intervals between current lines are marked. Enhancement of current density near the coastal line and the correlation between directions of a coastal and current lines are noticable (see text).

not be associated with the above-mentioned instability of field-aligned currents. One may assume that in this case a breakup was triggered by the ion tearing mechanism in the plasma sheet. Thus, both basic mechanisms proposed for description of the substorm breakup phase trigger probably do operate, but in substorms of different kinds. One still cannot rule out the possibility of their combined action.

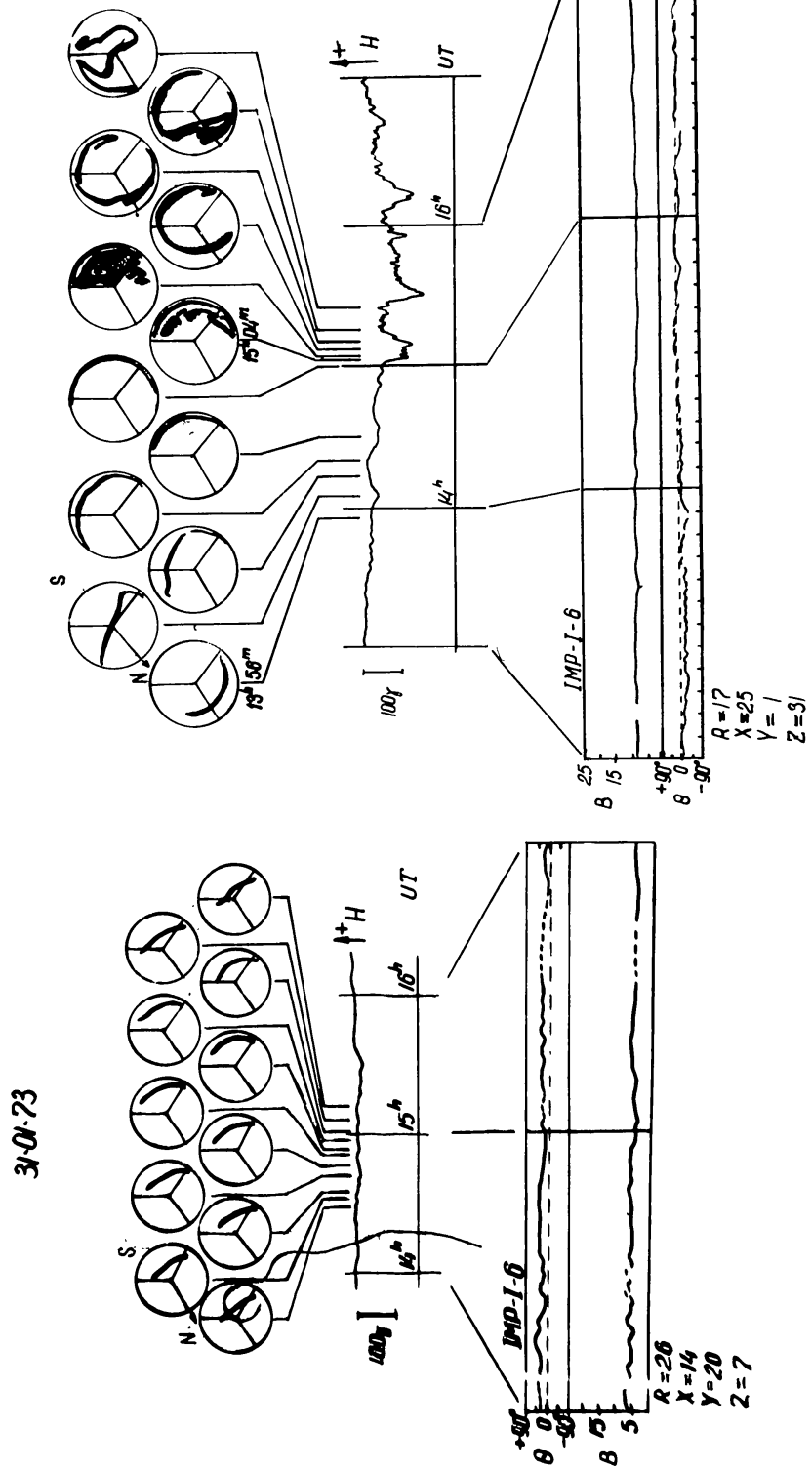

Fig. 31. Small substorms, having been recorded at Cape Golomjanaya ($\Phi \approx 74°$, $\Delta \approx 163°$) at the north (left) and south (right) IMF. *Top:* position of arcs, shown schematically. Arrows – direction to the geomagnetic pole; diameter of circles corresponds to 12° of latitude. *Middle: H*-magnetograms. IMF parameters and coordinates of IMP 1–6.

Ground-based data are presented by the courtesy of V. Parkhomov and R. Rakhmatulin, the satellite data – by Dr N. F. Ness.

We shall try to find out whether a scheme involving the plasma sheet reconnection is suitable enough for qualitative understanding of the above-mentioned coastal effects, the effect of patchiness and of the steplike electrojet expansion. We shall examine this problem first with reference to the patchiness effect.

The magnetic field inhomogeneities, producing, as noted, this effect, are small: ($\delta H/H \sim 10^{-2}$). Nevertheless, one can show (using, e.g., the estimations ($\delta H/H$), the duration of the plasma sheet thinning and breakup development processes) that a field tube with $\delta H > 0$ can be singled out as the first among others where the breakup process will commence and have enough time to develop. If the flux of particles thereby formed in the vicinity of the neutral line (in the plasma sheet portion, onto which a singled out field tube is projected) is capable of canceling (stopping) a thinning process of the surrounding plasma sheet, then the development of the breakup in space will be delayed for a considerable period ($\Delta\tau = 10^2$–10^3 s) of the tube depletion, which appears to be distinguished as a local breakup zone. It looks as if it takes place just in this manner. Indeed, Hardy *et al.* (1975) have shown that plasma sheet filling at the lunar orbit (during the substorm recovery phase) takes place mostly due to plasma generated near the neutral line. Since the characteristic time for thinning and thickening is comparable, it implies that an appreciable compensation of the thinning process by the plasma flow formed near the neutral line does take place, i.e. the regions of the initial breakup should be isolated for time $> \delta\tau$. This interval is probably increased due to plasma transport to the singled out field tube from the neighboring ones. Thus, the latter tubes will experience depletion with no breakup processes inside them. When the singled out tube exhausts itself as well, the breakup will be transferred (e.g. through the rarefaction wave (Coroniti and Kennel 1971)) deeper into the tail, i.e. to the region, separated from the singled out tube by the above adjacent region. Hence, the explosive development will take place in a steplike fashion.

5. Conclusions

Note the following results:

(1) It is shown that not only Z but Y and X-components of the IMF too have a strong effect on electric fields and currents in the quiet and disturbed magnetosphere.

The effects of IMF B_Z, described in the present work, do not differ from the known ones. They consist in the enhancement of the dawn–dusk electric field with increasing B_S and in the equatorward shift of the magnetospheric cleft and of the inner edge of the plasma sheet.

IMF B_Y produces in the polar caps a meridional electric field $\sim \mathbf{V} \times \mathbf{B}_Y$ and a dawn–dusk field $\sim |B_Y|$. The former has a sharp maximum (up to 50–100 mV m^{-1}) inside the ionospheric projection of the magnetospheric cleft; the latter is approximately twice as weak as the dawn–dusk field produced by the B_S-component

under condition $B_S = |B_Y|$. Thus, the field B_Y along with the IMF south component may be a cause of substorms.

IMF B_X rotates the ionospheric projection of the electric field $\mathbf{E} = \mathbf{V} \times \mathbf{B}$ through a considerable angle (up to 40°), depending on sign and value of B_X/B_Y.

All the above IMF effects qualitatively agree with the expected consequences of the reconnection hypothesis and are impressive confirmation of it. However, the value of the magnetospheric electric field appears to be almost an order less than the projected field $-\mathbf{V} \times \mathbf{B}$. Besides, these effects of module B_Y are found for a relatively small number of cases and in the presence of noise, comparable to the signal. Therefore, it is of no doubt that additional studies are required before final conclusions on the validity of the reconnection hypothesis can be reached.

(2) It is shown that a magnetospheric cleft (unlike the dayside polar cusp) is closed; its ionospheric projection has a quasi-circular shape and is located at $\Phi_c = 75$–$80°$ (*values* Φ_C are in the function of B_Z).

This zone of the magnetospheric cleft, closed at $\Phi \approx$ const., coincides with the zone of enhanced precipitation of particles with $W \lesssim 1$ keV.

In the ionospheric projection of the cleft a polar electrojet is flowing – a Hall current $\sim 10^2$ kA with zonal direction. At quiet time this electrojet is formed mainly due to focusing of the meridional component of the field $-\mathbf{V} \times \mathbf{B}_Y$ within $\Phi = 75$–$80°$. At disturbed periods an additional role is played by the enhancement of conductivity in the nightside portion of the cleft zone and by ionospheric closing currents of the westward auroral electrojet.

A quasi-circular shape of the magnetospheric cleft is qualitatively consistent with the one predicted in the reconnection model by Stern (1973).

(3) Distinct signatures of the *pre-breakup phase* of the magnetic substorm take place both at IMF $B_Z < 0$ and at $B_Z > 0$. The substorm onset is well observed 1.5–2 hours prior to the breakup inside the magnetospheric cleft zone. Then, independent of sign B_Z, the dawn–dusk electric field, polar and auroral electrojets are enhanced (2–4 times). The westward auroral electrojet develops along the morning part of the circular zone near $\Phi = 67°$. This zone corresponds to a projection of the drift shell of electrons generated near midnight ($W \approx 10$ keV and pitch-angles $\alpha < 45°$); the eastward electrojet develops along the spiral projection of the inner edge of the plasma sheet ($\alpha > 45°$).

It is likely that the reasons for enhancement of the magnetospheric convection and electrojets are not only electric fields $-\mathbf{V} \times \mathbf{B}_Z$ and $-\mathbf{V} \times \mathbf{B}_Y$.

A two-vortex convection system develops so that the enhancement of anti-solar convection in the boundary layer passes ahead of the return convection growth in the plasma sheet.

The evening sector appears to be distinguished 1.5–2 hours prior to the breakup in that the magnetic substorm onset is seen here at $\Phi = 75$–$80°$ but at the latitudes of a spiral, corresponding to the inner edge of the plasma sheet.

(4) Fine structure features of the explosive development of substorms are noted, which enable us to divide these substorms into two types. The trigger of

the breakup phase of the first kind is, evidently, the instability of field-aligned currents (Coroniti and Kennel 1972b); a specific feature for them is the expansion of the westward electrojet and magnetosphere–ionosphere interaction with a positive feedback (Oguti 1971; Atkinson 1970). The second kind of substorm trigger is probably instability like ion tearing (Schindler 1974; Galeev and Zeleny 1975).

(5) In the course of the analysis of the role of IMF B_S on magnetospheric electric fields a question was also raised about the contribution of the former to the generation of fields and currents of the dayside midlatitude ionosphere (S_q). This contribution is found to be $\lesssim 15\%$, i.e. the main source of S_q-fields is the ionospheric but not magnetospheric dynamo.

At the same time IMF B_s makes a considerable contribution to the S_q-field (10–20%), caused mostly by the field-aligned and ionospheric closing currents of a partial ring current.

Many results of this review are relatively new and probably will be improved in the course of the current International Magnetospheric Study.

In this connection it should be noted that after this review had been written a number of works were published which contain fundamental contributions to a general conception of magnetospheric storms. For their description a special review would be needed. I shall note shortly only some special results.

Russell (1976), Kokubun *et al.* (1976), on the basis of earlier results (e.g. Piddington 1963; Burch 1972; Russell *et al.*,1974) have shown that shock waves and other pressure waves in the interplanetary medium are not, per se, responsible for geomagnetic storms. The role of the pressure pulse is to compress the IMF. The substorms after such pulses (SSC, SI) take place only if the magnetosphere has been preconditioned by a period of southward IMF (growth phase or $AE \geqslant 100\gamma$).

On the other hand, it seems now that prolonged existence of southward IMF do not involve spasmodic substorms including large-scale re-configuration of the magnetosphere with neutral line formation in the tail (Pytte *et al.*, 1976a). In such periods the plasma in the tail flows continuously earthward (Hones *et al.*, 1976). At the same time prolonged existence of southward IMF corresponds to strong (up to $AE \sim 1000\gamma$) activity of a continuous type at high latitudes, generated by currents of DP-2-type. Such a current-system of the 'convection bay' involves a relatively weak westward auroral electrojet that corresponds only to weak positive H-bay in the evening sector of mid-latitudes. The continuous activity can generate the geomagnetic storm main phase (DR-current) without spasmodic substorms including the reconnection in the tail and strong AEJ (Russell 1976). It is also very probable that the 'well-known' kind of substorm spasmodic substorms – are triggered by not southward IMF but by decreasing the latter or by the change of IMF sign (Russell 1976). It is also probable that reconnection in the tail during such a substorm is the trigger but not the effect of a substorm because one can see the beginning of this process in the plasma sheet ~1 min before onset of the

substorm on the ground (Pytte *et al.*, 1976b). Sugiura and Potemra (1975), Iijima and Potemra (1976), Sarris *et al.* (1975) have also obtained additional important fragments on the new general substorm model.

So, one can see that in the current development of the substorm model there is a trend to join up different conceptions together with their modifications. For example, it is evident that the growth phase model has gotten new support and, at the same time, some more definite definitions (plasma-sheet thinning is not so important for convection bays as it was for substorm in the 'UCLA' model). On the other hand, if 'convection bays' are really not including nightside reconnection (at least as the trigger) that more corresponds to Akasofu's substorm model. Of course, the new facts mentioned above and their developments (it is also one of the important tasks of the IMS) must influence some of our conclusions (especially 4.2.2) but they perhaps allow the main sense to be preserved.

Acknowledgements

The author is grateful to his co-workers at SibIZMIR – A. Bazarzhapov, M. Matveev, V. Shelomentsev, T. Saifudinova, E. Nemtsova, E. Ponomarev, G. Shpynev, and L. Sergeeva for valuable discussions and help in computations. He is also indebted to I. Lazareva and I. Rabetskaya for their help in the design of this review. He is further grateful to Drs N. F. Ness, A. Nishida, W. Paulishak, and V. Golovkov for supplying satellite and ground-based magnetic data, and to Dr T. Pytte for his very informative and useful comments on the preprint of this review paper.

References

Akasofu, S.-I.: 1968, *Polar and Magnetic Substorms*, Dordrecht, Reidel, 354 pp.
Akasofu, S.-I.: 1972, *J. Geophys. Res.* **77,** 6275.
Akasofu, S.-I.: 1975a, *Planet. Space Sci.* **23,** 1349.
Akasofu, S.-I.: 1975b, Magnetic Storms and Substorms, Including Aurora-Magnetosphere Relations (Review), IAGA Div. III Rep. Rev.
Akasofu, S.-I. and Chapman, S.: 1972, *Solar-Terrestrial Physics*, Int. Ser. Monogr. Phys., S. I., Clarendon Press, Oxford Univ. Press, 891 pp.
Akasofu, S.-I. and Kane, J. R.: 1973, *Radio Sci.* **8,** 1049.
Akasofu, S.-I., Perreault, P. D., and Yasuchara, F.: 1973, *J. Geophys. Res.* **78,** 7490.
Aksenova, L. V., Matveev, M. I., and Mishin, V. M.: 1971, *Issled. po Geomagn., Aeron. i Fizike Solntsa*, **19,** 71.
Armstrong, J. C. and Zmuda, A.: 1970, *J. Geophys. Res.* **75,** 7122.
Atkinson, G.: 1970, *J. Geophys. Res.* **75,** 4746.
Atkinson, G.: 1972, in K. Folkestad (ed.), *Magnetosphere-Ionosphere Interactions*, Universitetsforlaget, Oslo, Norway, pp. 203–216.
Axford, W. I.: 1969, 'A Review of Fields and Particles in the Vicinity of the Synchronous Orbit', paper presented at the ESRO Colloquim, October, 1969.
Axford, W. I. and Hines, C. O.: 1961, *Can. J. Phys.* **39,** 1433.
Bassolo, V. S., Mansurov, S. M., and Shabansky, V. P.: 1972, *Issled. po Geomagn., Aeron. i Fizike Solntsa* **23,** 125.

Bazarzhapov, A. D., Mishin, V. M., and Nemtsova, E. I.: 1971, *Issled. po Geomagn., Aeron. i Fizide Solntsa* **19,** 87.
Bazarzhapov, A. D., Mishin, V. M., and Shpynev, G. B.: 1975, *Gerl. Beitr. Geophys.* **84,** 918.
Beljakova, S. I., Zaitseva, S. A., and Pudovkin, M. I.: 1968, *Geomagn. Aeron.* **8,** 712.
Birkeland, K.: 1908, *The Norwegian Aurora Polaris Expedition* 1902–1903, Vol. 1, 1-st Section, Christiania.
Burch, J. L.: 1972, *J. Geophys. Res.* **79,** 1105.
Burch, J. L.: 1973, *J. Geophys. Res.* **79,** 1105.
Burch, J. L.: 1974, *Rev. Geophys. Space Phys.* **12,** 363.
Clauer, C. R. and McPherron, R. L.: 1974a, *J. Geophys. Res.* **79,** 2898.
Clauer, C. R. and McPherron, R. L.: 1974b, *J. Geophys. Res.* **79,** 2811.
Coroniti, F. and Kennel, C. F.: 1971, *Magnetospheric Substorms*, UCLA preprint PPG-98, September 1971.
Coroniti, F. and Kennel, C. F.: 1972a, *J. Geophys. Res.* **77,** 3361.
Coroniti, F. and Kennel, C. F.: 1972b, *J. Geophys. Res.* **77,** 2835.
Coroniti, F. and Kennel, C. F.: 1973, *J. Geophys. Res.* **78,** 2837.
Coroniti, F., McPherron, R. L., and Parks, G. K.: 1968, *J. Geophys. Res.* **73,** 1715.
Crooker, N.: 1975, *Rev. Geophys. Space Phys.* **13,** 995.
Dungey, J. W.: 1961, *Phys. Rev. Lett.* **6,** 47.
Fairfield, D. H. and Mead, G. D.: 1975, *J. Geophys. Res.* **80,** 535–542.
Feldstein, Y. I. and Starkov, G. V.: 1970, *Planet. Space Sci.* **18,** 501.
Feldstein, Y. I., Sumaruk, P. V., and Shevnina, N. I. 1974, *Kosmich. Issled.* **11,** 155.
Fougere, P. F.: 1963, *J. Geophys. Res.* **68,** 1137.
Friis-Christensen, E., Lassen, K., Wilhjelm, J., Wilcox, J. M., Gonzalez, W., and Colburn, D. S.: 1972, *J. Geophys. Res.* **77,** 3371.
Friis-Christensen, E. and Wilhjelm, J.: 1974, 'Polar Cap Currents for Different Directions of the IMF in the *Y–Z* Plane', paper R-41, Det Danske Meteorol. Inst.
Fukushima, N.: 1969, *Rept. Ionos. Space Res. Japan* **23,** 219.
Galeev, A. A. and Zeleny, L. M.: 1975, *Zh. E. T. Ph.* **22,** 360.
Glushakov, M. L. and Samokhin, M. V.: 1974, *Geomagn. Aeron.* **14,** 584.
Gonzalez, W. D. and Mozer, F. S.: 1974, *J. Geophys. Res.* **79,** 4186.
Hardy, D. A., Freeman, J., and Hills, H. K.: 1975, 'Plasma Observations in the Magnetotail', preprint Dept. of Space and Astronomy Phys., Rice Univ., Houston, Tex., U.S.A.
Hargreaves, J. K., Chivers, J. A., and Axford, W. I.: 1975, *Planet. Space Sci.* **23,** 905.
Heppner, J. P.: 1972, *J. Geophys. Res.* **77,** 4877.
Hirasawa, T. and Nagata, T.: 1972, 'Constitution of Polar Substorm and Associated phenomena in the Southern Polar Region', Japanese Antarctic Res. Expedition, Scient. Reports, ser. A, NIO, Tokyo.
Hoffman, R. A.: 1970, 'Auroral Electron Drift and Precipitation: Cause of the Mantle Aurora', Preprint GSFC X-646-70-205, June 1970.
Hoffman, R. A. and Burch, J. L.: 1973, *J. Geophys. Res.* **78,** 2867.
Hones, E. W., Jr., Bame, S. J., and Asbridge, J. R.: 1976 *J. Geophys. Res.* **81,** 227.
Hones, E. W., Jr., Singer, S., Lanzerotti, L. J., Pierson, J. D., and Rosenberg, T. J.: 1971, *J. Geophys. Res.* **76,** 2977.
Iijima, T.: 1968 *Rep. Ionosph. Space Res. Japan* **22,** 295.
Iijima, T.: 1972a, *Rep. Ionosph. Space Res. Japan* **26,** 263.
Iijima, T.: 1972b, *Rep. Ionosph. Space Res. Japan* **26,** 149.
Iijima, T.: 1974, *Rep. Ionosph. Space Res. Japan* **28,** 69.
Iijima, T., Fukushima, N., and Kamide, Y.: 1968, *Rep. Ionosph. Space Res. Japan* **22,** 161.
Iijima, T. and Nagata, T.: 1968, *Rep. Ionosph. Space Res. Japan* **22,** 1.
Iijima, T. and Nagata, T.: 1972, *Planet. Space Sci.* **20,** 1095.
Iijima, T., and Potemra, T.: 1976, *J. Geophys. Res.* **81,** 2165.
Ivanov, K. G and Evdokimova, L. V.: 1975, *Geomagn. Aeron.***15,** 303.
Ivliev, D. Y., Pudovkin, M. I., and Zaitseva, S. A.: 1970, *Geomagn. Aeron.* **10,** 300.
Jørgensen, S., Friis-Christensen, E., and Wilhjelm, J.: 1972, *J. Geophys. Res.* **77,** 1976.
Kamide, Y.: 1974, *J. Geophys. Res.* **79,** 49.
Kane, R. P.: 1971, *J. Geophys. Res.* **76,** 8199.

Kisabeth, J. L. and Rostoker, G.: 1973, *J. Geophys. Res.* **78,** 5573.
Kokubun, S.: 1971, *Planet. Space Sci.* **19,** 697.
Kokubun, S., McPherron, R. L., and Russell, C. T.: 1976, UCLA Publication No. 1489.
Langel, R.: 1974, *J. Geophys. Res.* **79,** 2363.
Lezniak, T. W. and Winckler, J. R.: 1970, *J. Geophys. Res.* **75,** 7075.
Leontjev, S. V. and Lyatsky, W. B.: 1974, *Planet. Space Sci.* **22,** 811.
Lyatsky, W. B. and Maltsev, Y. P.: 1972, in *Geofyz. Issled. v zone polyarnych sijani*, Apatity, Polyarny Geofyz. Inst., pp. 74–86.
Lyatsky, W. B. and Maltsev, Y. P.: 1975, *Geomagn. Aeron.* **15,** 118.
Maeda, H.: 1966, *J. Geomagn. Geoelectr.* **18,** 173.
Malin, S. R. C. and Palumbo, A.: 1975, *Ann. Geophys.* **41,** 115.
Mansurov, S. M.: 1969, *Geomagn. Aeron.* **9,** 622.
Matsushita, S.: 1971, *Radio Sci.* **6,** 279.
Matsushita, S. and Balsley, B.: 1972, *Planet. Space Sci.* **20,** 1259.
Matveev, M. I.: 1974, *Issled. po Geomagn., Aeron. i Fizike Solntsa* **30,** 71.
Matveev, M. I. and Mishin, V. M.: 1975, *Issled. po Geomagn., Aeron. i Fizike Solntsa* **36,** 26.
McPherron, R. L.: 1970, *J. Geophys. Res.* **75,** 5592.
McPherron, R. L.: 1974, *EOS Trans. AGU* **55,** 994.
Mishin, V. M.: 1962, *Trudy IZMIRAN* **20**(30), 148.
Mishin, V. M. and Aksenova, L. V.: 1974, *IMF effect*, in *Voprosy Issled. Nizhney Ionosfery i Geomagnetosfery*, No. 3, Novosibirsk, p. 225.
Mishin, V. M. and Bazarzhapov, A. D.: 1966, *Geomagn. Issled.* **8,** 23.
Mishin, V. M., Bazarzhapov, A. D., Nemtsova, E. I., and Anistratenko, A. A.: 1975a, *Issled. po Geomagn., Aeron. i fizike Solntsa* **36,** 18.
Mishin, V. M., Bazarzhapov, A. D., Nemtsova, E. I., Popov, G. V., and Shelometsev, V. V.: 1975b, in *Substorms and Disturbances in Magnetosphere*, Leningrad, Nauka, pp. 191–202.
Mishin, V. M., Bazarzhapov, A. D., Saifudinova, T. I., Urbanovich, V. D., and Shelomentsev, V. V.: 1974, *Issled. po Geomagn., Aeron. i Fizike Solntsa* **30,** 107.
Mishin, V. M. and Grafe, A.: 1971, *Program and Abstract of the XV General Assembly IAGA*, Moscow.
Mishin, V. M., Matveev, M. I., and Nemtsova, E. I.: 1975c, 'Global Geomagnetic Effects of the Interplanetary Magnetic Field B_y, preprint SibIZMIR 11–75, Irkutsk.
Mishin, V. M. and Saifudinova, T. I.: 1968, in *Fizika Magnetosfery i Polyarnye Buri*, Irkutsk, issue 11, pp. 355–397.
Mishin, V. M., Samsonov, V. P., Popov, G. V., and Saifudinova, T. I.: 1971, *Issled. po Geomagn., Aeron. i Fizike Solntsa* **19,** 31.
Mishin, V. M., Samsonov, V. P., Saifudinova, T. I., and Kurilov, V. A.: 1970, *Issled. po Geomagn., Aeron. i Fizike Solntsa* **11,** 3.
Mishina, N. A.: 1970, *Issled. po Geomagn., Aeron. i Fizike Solntsa* **11,** 56.
Mohlmann, D. and Wagner, C.-U.: 1970, *J. Atmos. Terr. Phys.* **32,** 445.
Mozer, F. S., Gonzalez, W. D., Bogott, F., Kelley, M. C., and Schutz, S.: 1974, *J. Geophys. Res.* **79,** 56.
Murayama, T. and Hakamada, K.: 1975, *Planet. Space Sci.* **23,** 75.
Nadubovich, Y.: 1967, in *Results of Investigation according to International Geophys. Projects. Aurorae*, No. 14, Moscow, Nauka, p. 77.
Nagata, T. and Kokubun, S.: 1962, *Rept. Ionos. Space Res. Japan*, **16,** 256.
Nagata, T. and Mizuno, H.: 1955, *J. Geomagn. Geoelectr.* **7,** 69.
Nishida, A.: 1971, *Cosmic Electrodyn.* **2,** 350.
Nishida, A.: 1975, *Space Sci. Rev.* **17,** 353.
Nishida, A. and Hones, E. W.: 1974, *J. Geophys. Res.* **79,** 535.
Nishida, A., Iwasaki, N., and Nagata, T.: 1966, *Ann. Geophys.* **22,** 478.
Oguti, T.: 1969, *Rept. Ionos. Space Res. Japan* **23,** 175.
Oguti, T.: 1971, *Cosmic Electrodyn.* **2,** 164.
Osipova, I. L. and Vanjan, L. L.: 1975, *Geomagn. Aeron.* **15,** 847.
Piddington, J. H.: 1963, *Planet. Space Sci.* **II,** 1277.

Piddington, J. H.: 1964, *Space Sci. Rev.* **3,** 724.
Pytte T., McPherron, R. L., Hones, Jr., E. W., West, Jr., H. I.: 1976a, 'Multiple-Satellite Studies of Magnetospheric Substorms: Distinction between Polar Substorms and connection Driven Negativ Bays, January (a76)'. UCLA preprint, subnitted to *J. Geophys. Res.*
Pytte, T., McPherron, R. L. Kivelson, M. G., West, Jr., H. I., Hones, Jr., E. W.: 1976b, 'Multiple-Satellite Studies of Magnetospheric Substorms: Radial Dynamics of Plasma Sheet'. UCLA preprint, March 1976, submitted to *J. Geophys. Res.*
Pytte, T. and Trefall, H.: 1971, 'Auroral Zone Electron Precipitation Events Observed Before and at the Onset of Negative Magnetic Bays', paper presented at the XV IUGG General Assembly, Moscow, U.S.S.R.
Roederer, J.: 1974, *Science* **183,** 37.
Rostoker, G.: 1974, in B. M. McCormac (ed.) *Magnetospheric Physics*, D. Reidel Publ. Co., Dordrecht, p. 325.
Rostoker, G.: 1975, 'Magnetic Fields, Electric Fields and Current Systems, Including Ground Observations', IAGA Div. III Reporter Reviews.
Rostoker, G. and Kisabeth, J. L: 1973, *J. Geophys. Res.* **78,** 5559.
Russell, C. T.: 1974, *Solar Wind and Magnetosphere Dynamics*, 7-th ESLAB Symposium on Correlated Interplanetary and Magnetosphere Observations, D. Reidel Publ. Co., Dordrecht, Holland.
Russell, C. T., McPherron, R. L., and Burton, R. K.: 1974, *J. Geophys. Res.* **79,** 1105.
Russell, C. T.: 1976, 'R· connexion'. Paper presented at the STP Symposium, Boulder, Colo., June, 1976.
Samsonov, V. P.: 1971, *A Fine Structure of Space-Time Distribution of Aurorae*, Diss., Yakutsk, IKFiA.
Sarris, E. T., Krimigis, S., and Armstrong, T. P.: 1975, 'Observations of Magnetospheric Bursts of High Energy Protons and Electrons at 35 with IMR-7', preprint, Johns Hopkins.
Schindler, K.: 1974, *J. Geophys. Res.* **79,** 2803.
Sergeev, V. A.: 1973a, *Int. Ass. Geomagn. Aeron. Bull.* **34,** 458.
Sergeev, V. A.: 1973b, 'On Localization and Spatial Spreading of Particle Acceleration Region During Magnetospheric Substorm', Program and Abstracts for II IUGG General Assembly, Kyoto, September 1973, p. 458.
Sergeev, V. A.: 1974a, *Planet. Space Sci.* **22,** 1341.
Sergeev, V. A.: 1974b, 'The Descrete Activizations of Magnetosphere During Substorm Expansion Phase', Program and Abstracts of STP Symposium, Sao Paulo, Brazil, p. 49.
Shelomentsev, V. V.: 1974, *Issled. po Geomagn. Aeron. i Fizike Solntsa* **30,** 85.
Siscoe, G. L.: 1975, *Rev. Geophys. Space Phys.* **13,** 990.
Stern, D.: 1973, *J. Geophys. Res.* **78,** 7292.
Sugiura, M., and Poterma, T.: 1976, *J. Geophys. Res.* **81,** 2155.
Sumaruk, P. V. and Feldstein, Y. I.: 1973, *Kosmich. Issled.* **11,** 155.
Svalgaard, L.: 1968, 'Sector Structure of the Interplanetary Magnetic Field and Daily Variation of Geomagnetic Field at High Latitudes', paper R-6, Det Danske Meteorol. Inst.
Troitskaya, V. A. *et al.*: 1969, in *Solar-Terr. Physics*, Moscow, p. 234.
Troshichev, O. A., Kuznetsov, B. M., and Pudovkin, M. I.: 1974, *Planet. Space Sci.* **22,** 1403.
Vanjan, L. L. and Osipova, I. L: 1973, 'Electroconductivity of the Polar Ionosphere', preprint IKI, Moscow, 47 pp.
Vershinina, T. I.: 1966, *Geomagn. Aeron.* **6,** 365.
Vorobiev, V. G. and Rezhenov, B. V.: 1973, *Inst. Ass. Geomagn. Aeron. Bull.* **34,** 441.
Wiens, R. G. and Rostoker, G.: 1975, *J. Geophys. Res.* **80,** 2109.
Winningham, J. D., Yasuhara, F., Akasofu, S.-I., and Heikkila, W. J.: 1975, *J. Geophys. Res.* **80,** 3148.